Report

for the
Marshall Plan Scholarship supported research stay

at the
Laboratory of Enrique Rodriguez-Boulan,
Dyson Vision Research Institute,
Weill Cornell Medical College, NY

from 04/01/2010 to 10/01/2010

Roland Thünauer
PhD Student
at the
Institute for Biophysics, Johannes Kepler University Linz
and the
Center for Advanced Bioanalysis GmbH, Linz

Evaluated by
Prof. Peter Pohl
Institute for Biophysics, Johannes Kepler University, Linz

Table of Contents

Abstract

In the current project we adapted a system that allows to precisely regulate membrane trafficking (Rivera, Wang et al. 2000) to determine the role of the Rab11-compartment in Rhodopsin biosynthetic traffic to the apical plasma membrane in polarized epithelial cells. The system is based on conditional aggregation domains (CADs) fused to Rhodopsin-GFP. The resulting protein is retained in the ER until a membrane permeable drug, AP21998, is added that competes with the homo-association of the CADs. We found that both in non-polarized and polarized cells Rhodopsin is temporally co-localizing with the Rab11-compartment en route to the plasma membrane. Interestingly, the effect of a dominant negative version of Rab11 (Rab11-mCherry-S25N) depends on the polarization state of the cells. While in non-polarized cells Rab11-mCherry-S25N did not significantly interfere with Rhodopsin plasma membrane targeting, in polarized cells expression of Rab11-mCherry-S25N resulted in partial intracellular retention of Rhodopsin and basolateral mistargeting. Further we showed by TIRF microscopy that Rhodopsin vesicles undergoing fusion with the plasma membrane also carry Rab11. We observed that Rab11 is removed from the fusion site much quicker than Rhodopsin, suggesting a regulatory role of Rab11 in the vesicle fusion process. Monitoring vesicle fusion events at the apical membrane which was made possible for the first time by a PDMS-based biochip enabling apical TIRF microscopy shows a variety of different vesicle fusion behaviors, including non-radial spreading of the vesicular content after fusion. We observed that individual vesicle fusion sites are distributed all over the apical membrane.

Analogous observations for the role of Rab11 in biosynthetic membrane traffic have been made by investigating the apically targeted mutant CAR-Y318A of the Coxsackie virus and adenovirus receptor (CAR). While wt-CAR is targeted to basolateral plasma membrane, CAR-Y318A is re-routed to the apical plasma membrane. Only for CAR-Y318A the plasma membrane transport becomes Rab11-dependend in polarized MDCK cells.

Taken together, this data suggests that the Rab11 compartment matures to a specific state in polarized cells. In this state an apical sorting decision is made at this compartment that depends on the activity of Rab11.

Introduction and Background

Polarized epithelial cells

Epithelial cells form the outermost cell layer throughout the body of animals and humans. In virtually all organs epithelial cell layers function as barrier that separates the interior of an organ from the lumenal space filled with extracellular fluid (Rodriguez-Boulan, Kreitzer et al. 2005; Mellman and Nelson 2008). The permeability of this barrier layer is selectively regulated for defined species of molecules. Polarized epithelial cell layers can carry out vectorial transport of ions and solutes, i.e. they transport ions and solutes only into one direction, inwards or outwards of the organ. In order to carry out these functions polarized epithelial cells have a specialized architecture (see Figure 1). The main feature is that the plasma membrane is separated into two domains, the basolateral membrane (BM) and the apical membrane (AM). The separation of the membrane domains is maintained by the tight junctions (TJ) that also seal neighboring cells together. Polarized epithelial cells have adapted their membrane trafficking system to selectively insert a subset of membrane proteins solely to the apical membrane or to the basolateral membrane. The asymmetry or polarity of specialized transmembrane transporter proteins and channels allows the cell layer to carry out vectorial transport processes. A specialized trafficking machinery sorts proteins into basolateral and apical vesicular carriers that are selectively targeted to their respective target domain. The main branching point is believed to be the Trans Golgi Network (TGN) (Keller, Toomre et al. 2001). In some cases polarity can also be achieved by stabilizing a protein in one domain by interaction with the cytoskeleton and/or by a dedicated endocytosis machinery that quickly removes the protein from one compartment while it does not so from the other. An example is the Na/K-ATPase that can be targeted to both the apical and the basolateral membrane in MDCK cells but is stabilized selectively at the basolateral membrane thereby generating basolateral polarity (Hammerton, Krzeminski et al. 1991). Additionally, polarized epithelial cells have adapted the organization of the actin and microtubule cytoskeleton in order to perform directional membrane trafficking (Kreitzer, Schmoranzer et al. 2003).

As the current project is focused on the apical part of the membrane trafficking system an overview about apical membrane trafficking mechanisms and routes is given in the next chapter.

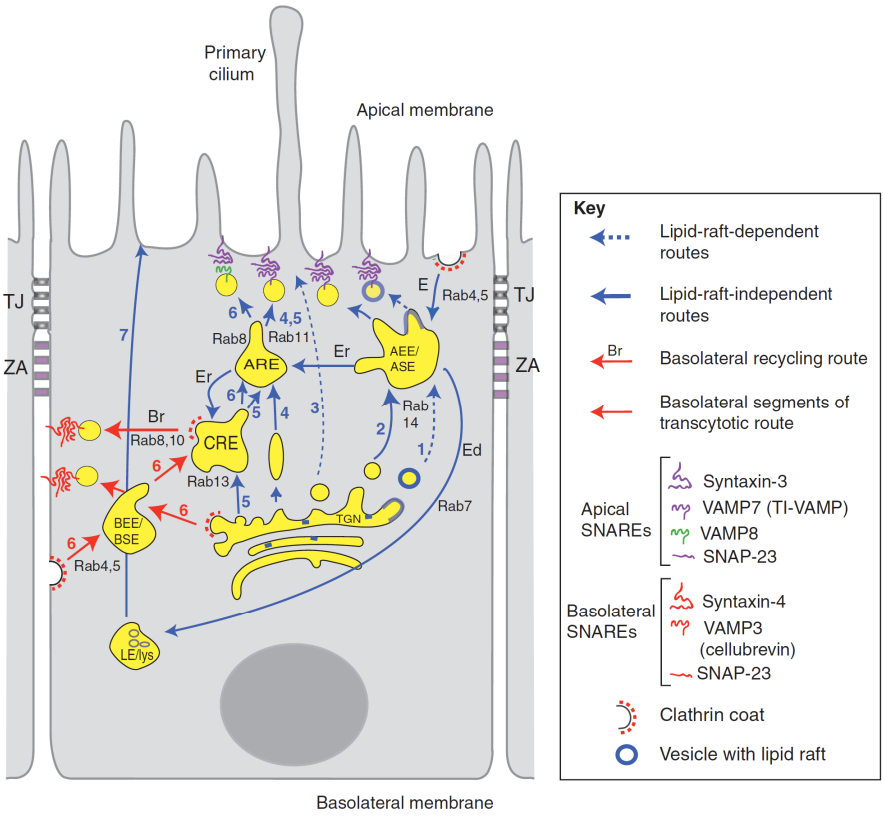

Figure 1: Architecture and apical membrane trafficking system of a polarized epithelial cell. *(taken and adapted from (Weisz and Rodriguez-Boulan 2009))*

Routes to and from apical plasma membrane domains are shown in blue. For comparison, some of the basolateral routes are shown in red. AEE…apical early endosome, ARE…apical recycling endosome, ASE…apical sorting endosome, BEE…basolateral early endosome, Br…basolateral recycling, BSE…basolateral sorting endosome, CRE…common recycling endosome, Er…endosome recycling, Ed…endosome degradation, LE…late endosome lys…lysosome, TGN…trans Golgi network, TJ…tight junction, ZA…zonula adherens.

Route 1: Route for lipid-raft-associated proteins.

Route 2: Rhodopsin is the only protein that might follow this route in order to reach the primary cilium.

Route 3: Hypothetical direct route of raft-associated proteins to the primary cilium.

Route 4: The non-raft-associated proteins p75 and sialomucin endolyn follow this route.

Route 5: An apical variant of the VSVG protein is thought to use this route.

Route 6: The pIgR is first inserted into the basolateral membrane and then transcytoses to the apical membrane.

Route 7: Specific types of exosomes can be exocytosed apically.

Apical membrane traffic

A proper function of the apical membrane trafficking system is vital for the whole organism. Several diseases, including the microvillus inclusion disease, cystic fibrosis and retinitis pigmentosa have been related to malfunctions of the apical trafficking system (Mellman and Nelson 2008). While the diseases can also be caused by mutations that render a pivotal apical membrane protein nonfunctional, in most cases the protein itself remains functional but is not inserted correctly into the apical membrane by a defective apical trafficking machinery.

Therefore it is worthwhile to take a closer look at the apical trafficking system (see Figure 1). An immediately apparent and interesting aspect of apical membrane traffic (and also basolateral membrane traffic) is that there are many different routes that lead to the apical membrane. The routes are used by different subsets of proteins. The detailed reason for the multiple routes is not yet completely understood (Weisz and Rodriguez-Boulan 2009), possible causes are thought to be:

- *Flexibility:* The cell needs to regulate the membrane concentration of different subsets of membrane proteins independently in order to efficiently adapt to changing environmental conditions.
- *Sorting Signals:* Apical proteins have to exhibit, in order to be recognized by the apical sorting machinery, so-called sorting signals that are embedded in the protein structure. It has been established be extensive studies during the recent years that there exist many classes of apical sorting signals (Kreitzer, Schmoranzer et al. 2003; Rodriguez-Boulan, Kreitzer et al. 2005; Weisz and Rodriguez-Boulan 2009). Apical sorting signals include N- and O-linked glycans, glycosyl phosphatidylinositol (GPI) and transmembrane anchors, and amino-acid stretches in the cytoplasmic domain. Also the lipid raft hypothesis is thought to explain segregation and sorting of apical proteins based on their affinity for membrane domains enriched with sphingolipids and cholesterol (Brown and London 1998). For a detailed listing of apical sorting signals see (Weisz and Rodriguez-Boulan 2009).

An important emerging concept is that almost all proteins traverse endocytic compartments after leaving the TGN but before arriving at the plasma membrane. The reasons for this detour are not yet completely understood (Rodriguez-Boulan,

Kreitzer et al. 2005; Cramm-Behrens, Dienst et al. 2008; Farr, Hull et al. 2009; Weisz and Rodriguez-Boulan 2009) but may include:

- *Additional Sorting:* In addition to the sorting that occurs at the TGN, a refinement of sorting might occur during the passage through endocytic compartments.
- *Vesicular storage pools:* Cells can retain a fraction of channels or transporters in intracellular vesicular storage pools that can be inserted quickly into the plasma membrane upon extracellular stimulation. Examples include the water channel Aquaporin 2 (Brown 2003; King, Kozono et al. 2004) and the glucose transporter GLUT4 (Kessler, Tomas et al. 2000; Bryant, Govers et al. 2002).
- *Signaling nodes during establishment of polarity:* The intermediate compartments may serve as platforms where extracellular polarity cues and signals are integrated during establishment of polarity (Bryant, Datta et al. 2010).

Every endocytic compartment is marked by at least one marker protein. In the current project we were focusing on the apical recycling endosomal (ARE) compartment which is labeled predominantly by Rab11.

Rab11

Rab11 is a member of the Rab family of Ras-like small monomeric GTPases. Rab proteins are implicated in the regulation of various membrane transport steps (Zerial and McBride 2001). Rab11 can exist in an active, GTP-bound state and an inactive GDP-bound state. The GDP-bound form of Rab11 localizes mainly to the cytosol, in contrast to GTP-bound form. Several proteins (GTPase activator proteins (GAPs) and guanine nucleotide-exchange factors (GEFs)) regulate the cycling of Rab11 between the GTP- and GDP-bound states. However, to date no Rab11-specific GEFs and GAPs have been identified. Like other Rab GTPases, Rab11 in its active GTP-bound state interacts with various proteins, known as Rab11 effectors, including a family of Rab11-interacting proteins (Rab11-FIPs) (Hales, Griner et al. 2001). Rab11 can regulate vesicular trafficking via interaction with Rab11-FIPs that are believed to form scaffolding complexes and can also bind other membrane transport proteins.

In non-polarized cells Rab11 localizes to the pericentriolar compartment and is required for the transport of proteins in the biosynthetic (Chen, Feng et al. 1998) as well in the recycling route (Ullrich, Reinsch et al. 1996) of membrane traffic. During establishment of cell polarity Rab11 is a key part of the signaling network that regulates the formation of the apical surface and lumen (Bryant, Datta et al. 2010).
In fully polarized epithelial cells the Rab11 compartment adapts to the split trafficking system (Rodriguez-Boulan, Kreitzer et al. 2005). Rab11 plays a role in recycling from the apical membrane (Casanova, Wang et al. 1999; Prekeris, Klumperman et al. 2000; Wang, Kumar et al. 2000). Many apical proteins, presumably those not depending on detergent resistant membrane mediated sorting (Cresawn, Potter et al. 2007), pass through the Rab11 compartment en route to the plasma membrane (Cramm-Behrens, Dienst et al. 2008). As an interesting exemption, the basolateral protein E-cadherin has been identified to also pass through the Rab11 compartment (Lock and Stow 2005; Desclozeaux, Venturato et al. 2008) demonstrating that Rab11 can also be implicated in trafficking to the basolateral membrane.

Rhodopsin

In the current project we chose Rhodopsin as primary model molecule for our studies. Rhodopsin forms the light sensitive element of the visual system and is trafficked vectorially from the endoplasmic reticulum (ER) to the outer segment of mammalian photoreceptor cells (Tai, Chuang et al. 1999; Sung and Chuang 2010) that is reminiscent of the primary cilium in polarized epithelial cells. The transport of Rhodopsin to its target membrane is powered by direct binding to the light chain Tctex-1 of the motor protein dynein (Tai, Chuang et al. 1999). Thereby Rhodopsin-bearing vesicles are carried by dynein along microtubules. Remarkably, the sorting signals present at the Rhodopsin molecule, i.e. the Tctex-1 binding sequence, causes targeting to the apical membrane in polarized epithelial cells, like Madin-Darby canine kidney (MDCK) cells (Tai, Chuang et al. 2001). MDCK cells have proven to be a useful model system as both cell types, MDCK and photoreceptor cells, employ similar Rhodopsin trafficking mechanisms (Chuang and Sung 1998) but MDCK cells are much easier to culture and handle.
However, the understanding of the Rhodopsin trafficking route to the target membrane is incomplete (Weisz and Rodriguez-Boulan 2009; Sung and Chuang 2010). Data from Drosophila melanogaster suggests that Rab11 and the associated

compartment play an important role in Drosophila Rhodopsin trafficking (Satoh, O'Tousa et al. 2005; Wu, Mehta et al. 2005; Li, Satoh et al. 2007). But interestingly Drosophila Rhodopsin has no Tctex-1 binding sequence (Kock, Bulgakova et al. 2009). How the situation looks like in a mammalian system remains to be determined.

Apical TIRF microscopy and real time recording of vesicle fusion events

The last step in vesicular transport to a target membrane is the fusion of the vesicle with the target membrane itself. With confocal microscopy vesicles can be monitored to be transported to the plasma membrane and also to co-localize with the target membrane, but only a course verification if vesicles are undergoing fusion is possible because of lacking resolution (Kreitzer, Schmoranzer et al. 2003). The situation becomes even more complicated at the apical membrane of polarized MDCK cells that is intensively decorated by microvilli (Rodriguez-Boulan, Kreitzer et al. 2005), finger-like membrane evaginations with roughly 100 nm in diameter and 1 µm in length. Here, a light microscopy method with higher resolution is required to monitor individual vesicle fusion events. An excellent alternative is total internal reflection fluorescence (TIRF) microscopy. It allows studying the fate of vesicles close to the plasma membrane including vesicle fusion (Steyer, Horstmann et al. 1997; Schmoranzer, Goulian et al. 2000; Toomre, Steyer et al. 2000; Kreitzer, Schmoranzer et al. 2003). TIRF microscopy utilizes an exponentially declining evanescent wave that only excites fluorophores within 100 nm vicinity above a glass cover slip. Considering this parameters can be defined to unambiguously distinguish vesicle fusion events from other vesicular movements (Schmoranzer, Goulian et al. 2000). Figure 2 shows an example of a fusion event of a vesicle carrying the protein aquaporin-5 fused to green fluorescent protein (AQP5-GFP). For analysis a 2-dimensional symmetrical Gaussian distribution was fitted to the diffraction limited and then spreading spot representing the fusing vesicle. For a vesicle fusion event the time course of three parameters describing the Gaussian show a characteristic time dependence: The (with)² of the Gaussian, which is proportional to the area of the spot, increases linearly, the volume of the Gaussian representing the total intensity stays constant and the amplitude of the Gaussian representing the peak intensity decays exponentially as the cargo diffuses freely in the membrane after fusion. With

these parameters the qualitative changes upon fusion can be followed quantitatively (Figure 2B): Upon fusion onset (~0.6 s) the total intensity, and also the peak intensity, increased sharply, because the vesicle approached regions with higher excitation intensity within the evanescent wave. AQP5-GFP molecules subsequently spread via diffusion in the apical membrane, which was characterized by a linear increase of the spot area and an exponential decrease of the peak intensity. The linear increase in spot area corresponds to a diffusion coefficient of $1.4 * 10^{-10}$ cm^2/s, which is in good agreement with values for membrane proteins diffusing freely in the plasma membrane (Crane and Verkman 2008).

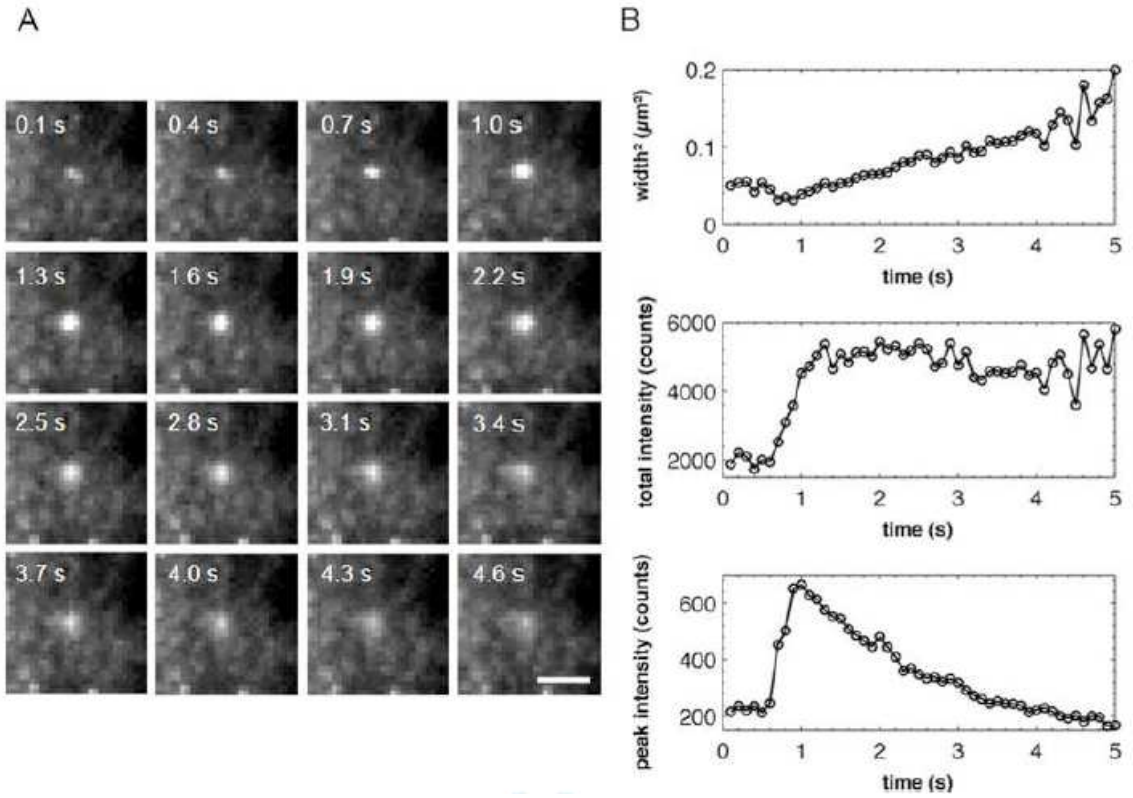

Figure 2. Vesicle fusion event at the plasma membrane as recorded by TIRF microscopy

(A) Image sequence of a vesicle fusion event recorded at the plasma membrane. For measurement a 20 °C Golgi exit block was applied to accumulate AQP5-GFP in the Golgi. In order to trigger plasma membrane trafficking of AQP5-GFP the Golgi exit block was released by re-heating to 37 °C after the cells had been transferred to the microscope. Pre-existing AQP5-GFP signal at the apical membrane was removed by bleaching followed by imaging of vesicle fusion events with a CCD-camera. The scale bar corresponds to 2 µm. (B) Time dependence of total intensity, peak intensity and width^2 of a Gaussian fitted to

the initially diffraction limited and then spreading fluorescence signal of the vesicle in A. The fusion event was identified by the characteristic time dependence of the three parameters shown: The volume of the Gaussian representing the total intensity stayed constant, while the amplitude of the Gaussian representing the peak intensity decayed exponentially. The (with)^2 of the Gaussian, which is proportional to the area of the spot, increased linearly upon fusion.

However, because of optical prerequisites (an evanescent wave can only be created at the low refractive index side by total internal reflection at an interface between to optical media with different refractive index) TIRF microscopy has been traditionally limited to study the basal plasma membrane that is attached to the glass support (Axelrod 2001; Steyer and Almers 2001). To overcome this limitation, a strategy that allows performing TIRF microscopy also at the free apical membrane has been developed during my ongoing PhD thesis at the Center for Advanced Bioanalysis. This was made possible by polydimethylsiloxane (PDMS) based biochips that carry an attached polarized cell monolayer and include an integrated positioning system. We developed two versions of the apical TIRF chip; with both versions polarized cells can be positioned in way that they dive with their apical membrane into the region of the evanescent wave above a glass cover slip on an objective-type TIRF microscope. The cell growth on the chips was restricted to defined cell growth areas that have been coated with fibronectin, an extracellular matrix protein that supports cell attachment to hydrophobic PDMS surfaces (Tan, Oldenburg et al. 2006; Tenstad, Tourovskaia et al. 2010). In a first step we verified that MDCK cells growing on fibronectin coated PDMS surfaces form a polarized monolayer by immunostaining for various apical and basolateral marker proteins (see Figure 3). As shown in Figure 3A the basolateral marker protein E-cadherin (Capaldo and Macara 2007; Deborde, Perret et al. 2008) localizes correctly to the basolateral membrane. Figure 3B shows that also the apical marker protein gp135 (Bryant, Datta et al. 2010) is restricted to the apical membrane. The cell monolayer displays intact tight junctions as shown by the localization of the tight junction associated protein ZO1 (Figure 3C). Also the exogenously expressed apical marker protein AQP5-GFP (Wellner and Baum 2001; Nejsum and Nelson 2007) shows correct apical localization (Figure 3C).

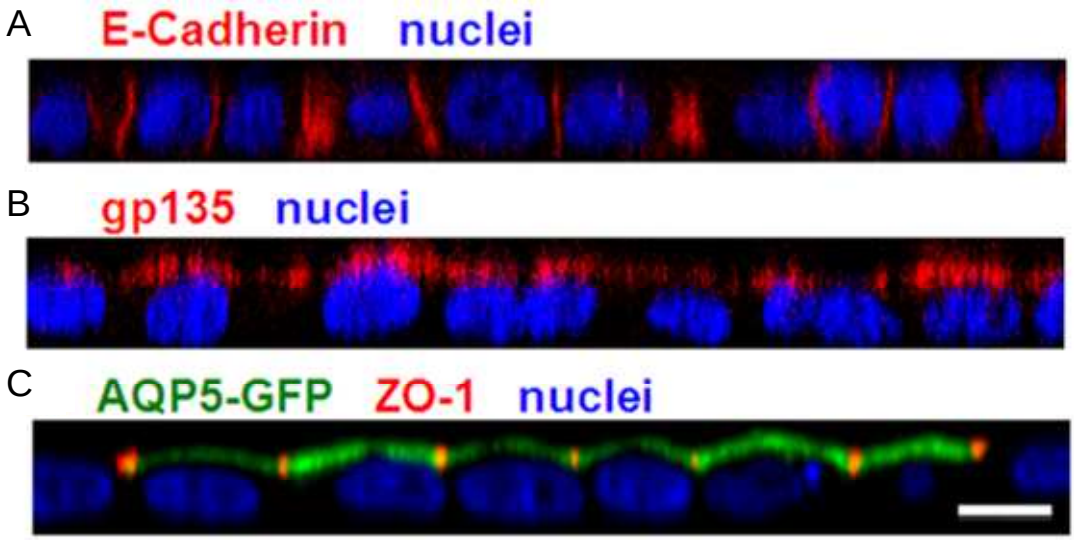

Figure 3. Localization of polarity marker proteins in MDCK cells grown for 4 days on fibronectin coated PDMS surfaces.

The subcellular localization of marker proteins was visualized with confocal microcopy; vertical cross sections through the cell monolayer are shown with nuclei in blue. Cells have a height of approximately 10 µm. The scale bar corresponds to 10 µm. (A) The endogenous basolateral marker protein E-cadherin (shown in red) localizes to the lateral regions of the plasma membrane. (B) The endogenous apical marker protein gp135 (shown in red) localizes to the apical plasma membrane. (C) AQP5-GFP (shown in green) transiently expressed in MDCK cells is targeted to the apical plasma membrane. The localization of ZO-1 (shown in red) indicates the correct formation of tight junctions.

Version 1 of the apical TIRF biochip

The design of the version 1 of the chip is schematically outlined in Figure 4A. Main parts of the chip are the actuator channels and the central cell growth area, which is coated with fibronectin. In a first step cells were seeded on top of the chip and cultured on the cell growth area in a drop of growth medium till a polarized cell monolayer was formed (Figure 4B). For apical TIRF imaging the actuator channels were pressurized causing the covering thin and elastic PDMS membrane to bulge outwards. The whole chip carrying the cells was placed upside down on a suitable glass cover slip at an inverted microscope. Finally, the pressure in the actuator channels was adjusted such that the cells moved with their apical membrane into the evanescent field of a totally internally reflected laser beam (Figure 4C).

Version 2 of the apical TIRF biochip

The design of the version 2 of the chip is schematically outlined in Figure 5A. The function principle is similar to the version 1 of the chip, but in the version 2 a piece of PDMS is attached to the actuator channels. This piece, that carries here the cell layer, can be moved in and out by the actuator channels like a stamp. In a first step cells were seeded on top of the chip and cultured on the cell growth area in a drop of growth medium till a polarized cell monolayer was formed (Figure 5B). For apical TIRF imaging the actuator channels were pressurized causing the central PDMS piece to move out. The whole chip carrying the cells was placed upside down on a suitable glass cover slip at an inverted microscope. Finally the pressure in the actuator channels was adjusted such that the cells moved with their apical membrane into the evanescent field of a totally internally reflected laser beam (Figure 5C).

Both versions of the chip were subjected to extensive practical testing at the microscope setup that has been established during the research stay at the Rodrigruez-Boulan lab.

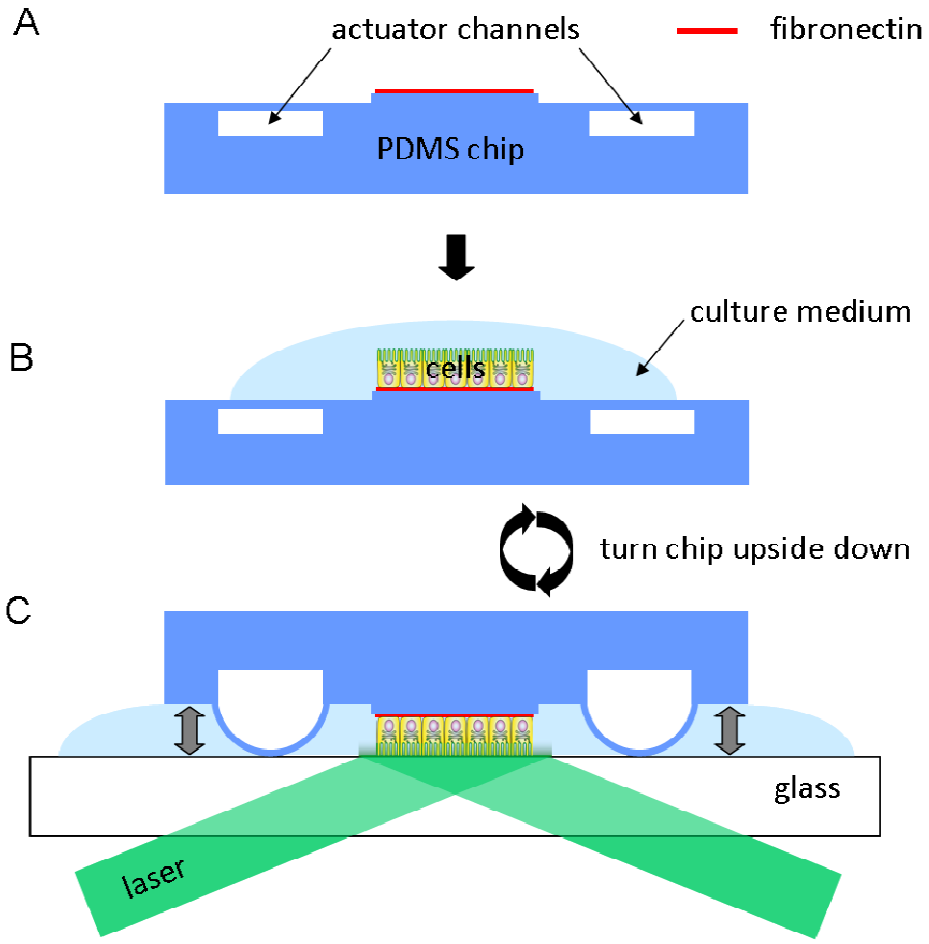

Figure 4. Operation principle of the version 1 of the PDMS biochip for apical TIRF microscopy

The biochip, made of PDMS contained integrated actuators channels for positioning. (A) In a first step the elevated cell growth area was coated with fibronectin (shown in red). (B) Cells were seeded on the chip in a drop of media and cultured till polarized. (C) For TIRF microscopy of the apical membrane the actuators were moved out and the whole chip was turned upside down and placed on a glass cover slip. The polarized cell monolayer was then approached to the glass cover slip such that the cells moved with their apical membrane into the evanescent field of a totally internally reflected laser beam coupled in through a high numerical aperture objective.

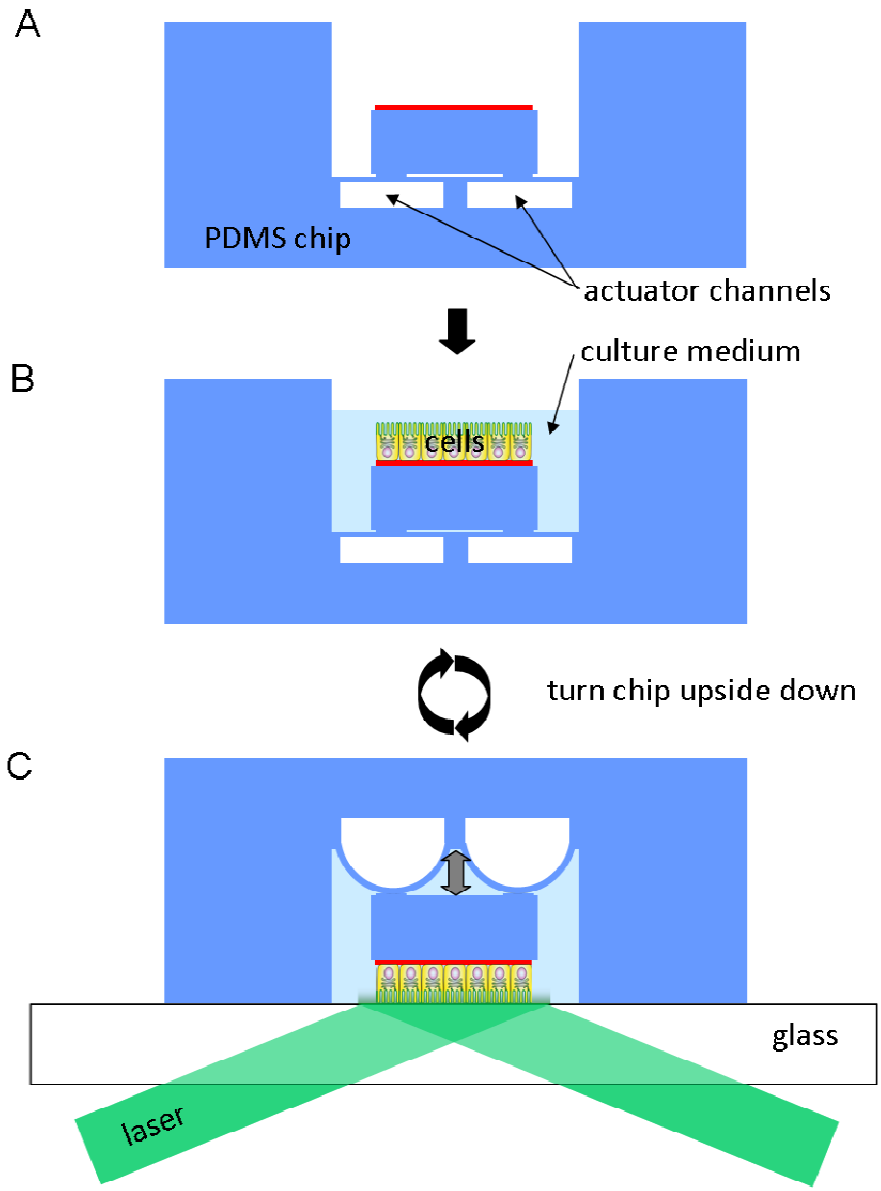

Figure 5. Operation principle of the version 2 of the PDMS biochip for apical TIRF microscopy

The biochip, made of PDMS contained integrated actuators channels for positioning. (A) In a first step the cell growth area was coated with fibronectin (shown in red). (B) Cells were seeded on the cell growth area and cultured till polarized. (C) For TIRF microscopy of the apical membrane the actuators and the attached central PDMS piece were moved out and the whole chip was turned upside down and placed on a glass cover slip. The polarized cell monolayer was then approached to the glass cover slip such that the cells moved with their apical membrane into the evanescent field of a totally internally reflected laser beam coupled in through a high numerical aperture objective.

Methods for imaging constitutive membrane traffic

One important practical consideration remains to be mentioned: In order to be able to image the passage of proteins through intracellular compartments it is necessary to pulse a synchronized cohort of labeled protein through the biosynthetic pathway.

Existing approaches rely on the 20°C Golgi exit block (Schmoranzer, Goulian et al. 2000; Keller, Toomre et al. 2001; Kreitzer, Schmoranzer et al. 2003) where the protein of interest is accumulated in the Golgi until released to the plasma membrane by reheating to 37°C. This approach has several disadvantages. It has been observed that the Golgi enlarges significantly during a 20°C block (Ladinsky, Wu et al. 2002), a situation that might interfere with normal Golgi function. Although the cells typically recover quickly after reheating from 20°C, it is not known if the temperature switching disturbs other cellular functions. An other limitation is that different proteins react differently to a 20°C Golgi exit block, so that it is difficult to achieve simultaneous release of two species of proteins.

These disadvantages can be overcome by a system presented in (Rivera, Wang et al. 2000). In this system the protein of interest is fused to conditional aggregation domains (CADs) that allow a retention in the endoplasmic reticulum (ER) until a reagent (AP21998) is added.

In the current project we adapted this system to enable imaging of biosynthetic membrane trafficking in polarized MDCK cells.

Goals

For the 6 months research stay at the Rodriguez-Boulan lab the following goals are defined:

Methodological/Practical goals

- Installation of a microscopy system that allows to perform high-speed multicolor confocal microscopy and multicolor TIRF microscopy
- Practical testing of the two versions of the biochip for apical TIRF microscopy
- Development of a protocol that allows to image membrane trafficking in polarized Madin-Darby canine kidney (MDCK) cells based on a regulated trafficking system

Biological/Scientific goals

- Investigation of the membrane trafficking route of Rhodopsin in polarized and non-polarized MDCK cells
    - Clarifying the role of endocytic compartments, especially the subapical Rab11 compartment (also known as apical recycling compartment (ARE))
    - Recording apical fusion events of Rhodopsin-bearing vesicles in order to characterize the fusion events in terms of topographic distribution at the apical membrane.
- Investigation of the membrane trafficking route of the apically targeted mutant CAR-Y318A of the Coxsackievirus and adenovirus receptor (CAR).

Results

Regulated trafficking system

We designed a plasmid that encodes a modified version of Rhodopsin, FM4-Rhodopsin-GFP, which trafficking out of the ER can be regulated by a system that is based on the approach described in (Rivera, Wang et al. 2000). The architecture of the construct is outlined in Figure 6A. Most N-terminal is the signal sequence of the human growth hormone (SS) which ensures that the ribosome synthesizing the protein is recruited to a translocon at the ER. The signal sequence is followed by four repeats of FM domains. The FM domains are a mutant version of the FKBP protein (Rivera, Wang et al. 2000) and have an intrinsic homo-association affinity and serve as conditional aggregation domains. Next is a furin cleavage site (FCS) and then protein of interest, Rhodopsin. After a sequence encoding for the green fluorescent protein (GFP) a sequence repeatedly encoding for the eight most C-terminal amino acids of Rhodopsin (RC) is attached. This ensures that the resulting protein still can bind to the dynein light chain Tctex-1 which is necessary for Rhodopsin apical transport (Yeh, Peretti et al. 2006). Figure 6B shows the membrane topology of the FM4-Rhodopsin-GFP construct.

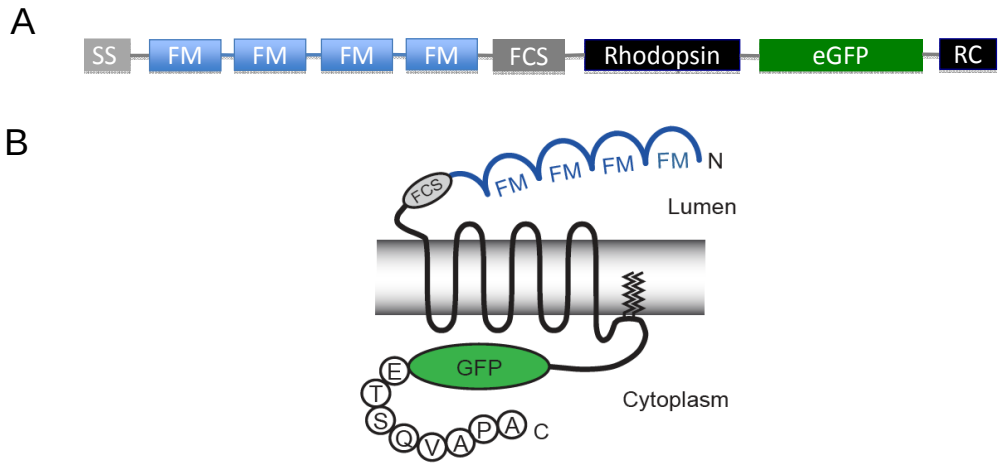

Figure 6. Architecture of the FM4-Rhodopsin-GFP construct.

(A) Protein domains encoded by the plasmid pFM4-Rhodopsin-GFP.

(B) Membrane topology of FM4-Rhodopsin-GFP. At the lumenal side four FM domains, enabling conditional aggregation, are fused to Rhodopsin, via a furin cleavage site (FCS). The cytoplasmic C-terminus of Rhodopsin is fused to GFP followed by a repeat of the extreme C-terminal Tctex-1 binding sequence of Rhodopsin.

SS… Signal sequence, RC… repeat of the extreme C-terminal of Rhodopsin

If the protein FM4-Rhodopsin-GFP was expressed in MDCK cells, it first accumulated in the ER (see Figure 7A and 7B, 0min) because the four FM domains induce association into large aggregates that are retained in the ER by the ER-quality control machinery (Rivera, Wang et al. 2000). These aggregates could be dissolved within minutes upon addition of the membrane permeable drug AP21998 that competes with the homo-association of the FM-domains. Within 10-15 min the bulk of FM4-Rhodopsin-GFP localizes to the Golgi (see Figure 7A and 7B, 15min). The protease furin which localizes predominantly to the Trans-Golgi (Simmen, Nobile et al. 1999) cleaves FM4-Rhodopsin-GFP at the FCS ensuring that only the native Rhodopsin is trafficked along the further biosynthetic pathway to the plasma membrane (Figure 7A, 120min and Figure 7C). As a further control we ensured that FM4-Rhodopsin-GFP is targeted to the apical plasma membrane in polarized MDCK cells (see Figure 8). For comparison the basolateral targeting of FM4-NCAM-GFP, a regulate-able variant of the neural cell adhesion molecule (NCAM) (Le Gall, Powell et al. 1997; Deborde, Perret et al. 2008) is also shown in Figure 8.

For all experiments MDCK II cells were transfected for 5-6 h with FM4-Rhodopsin-GFP using Lipofectamine 2000 (Tucker, Varga et al. 2003) which yielded sufficient transfection efficiency even for polarized filter grown cells. This time was long enough for the cells to synthesize sufficient amounts of protein but also short enough that no significant leakage out of the ER was evident. In order to be able to clearly follow a synchronized cohort of protein, further protein synthesis was abrogated by 100 µg/ml cycloheximide. In case of polarized cells filters were cut out and placed upside down on a glass cover slip on the microscope in recording medium containing AP21998 and cycloheximide. The filter piece was stabilized by placing a cloning cylinder on top.

Taken together this approach enables to image a synchronized cohort of labeled protein transported along the biosynthetic trafficking pathway of polarized MDCK cells.

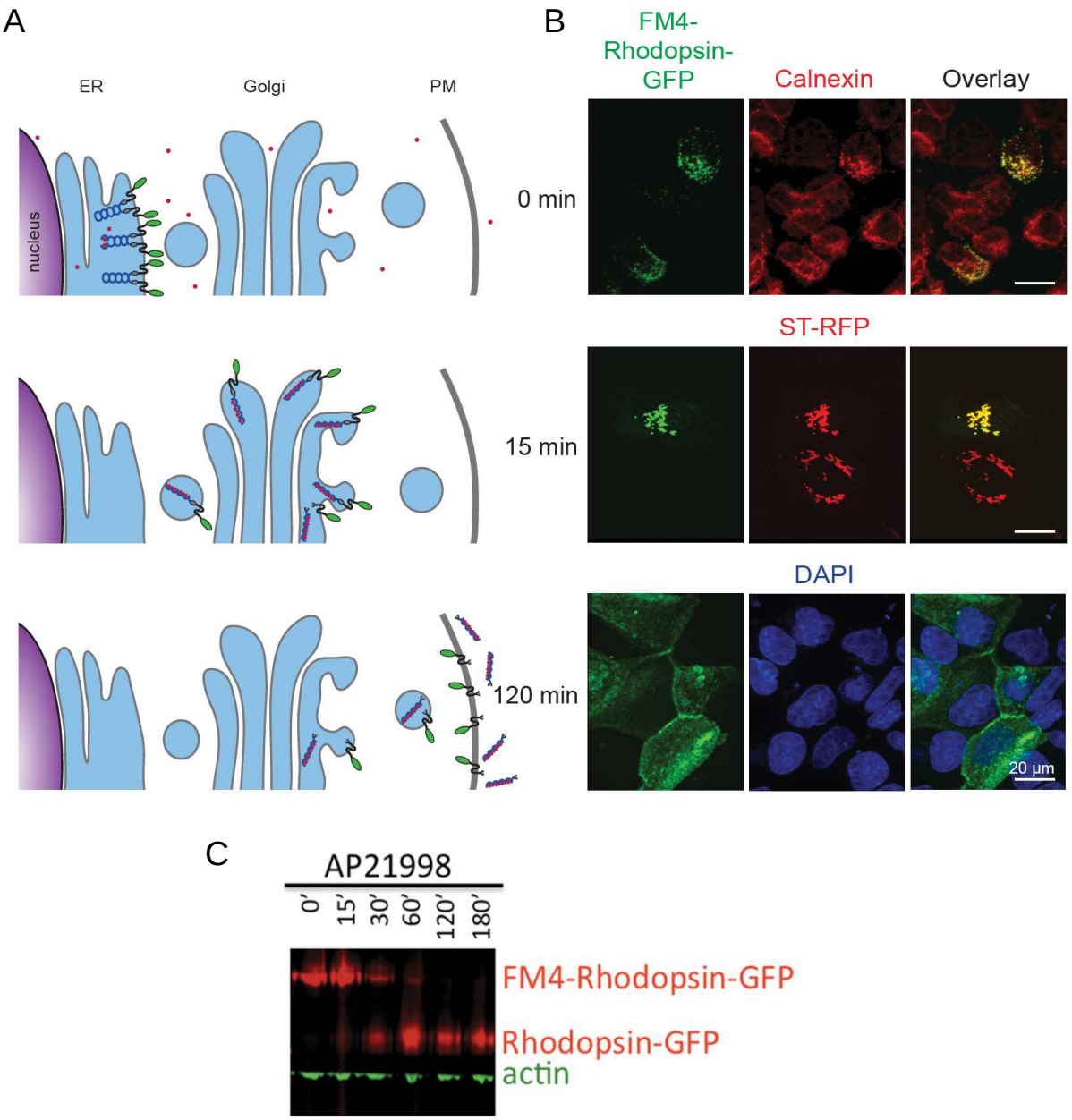

Figure 7. Functional principle of the regulated trafficking system for FM4-Rhodopsin-GFP

(A) Schematic illustration of the trafficking route and modifications of FM4-Rhodopsin-GFP occuring after release from the ER. As seen in (B), at 0 min, before addition of the release drug AP21998, FM4-Rhodopsin-GFP localizes to the ER as demonstrated by co-colocalization with the ER-marker calnexin. 15 min after release the majority of FM4-Rhodopsin-GFP is found at the Golgi as shown by co-localization with the Golgi-marker ST-RFP. After sufficient time (120 min) the majority of FM4-Rhodopsin localizes to the plasma membrane. The scale bar corresponds to 20 µm.

(C) FM4-Rhodopsin-GFP gets cleaved at the furin cleavage site if released from the ER upon addition of AP21998. The Figure shows a Western Blot of cell lysates from non-

polarized MDCK cells transfected with FM4-Rhodopsin-GFP and treated with AP21998 for the indicated times.

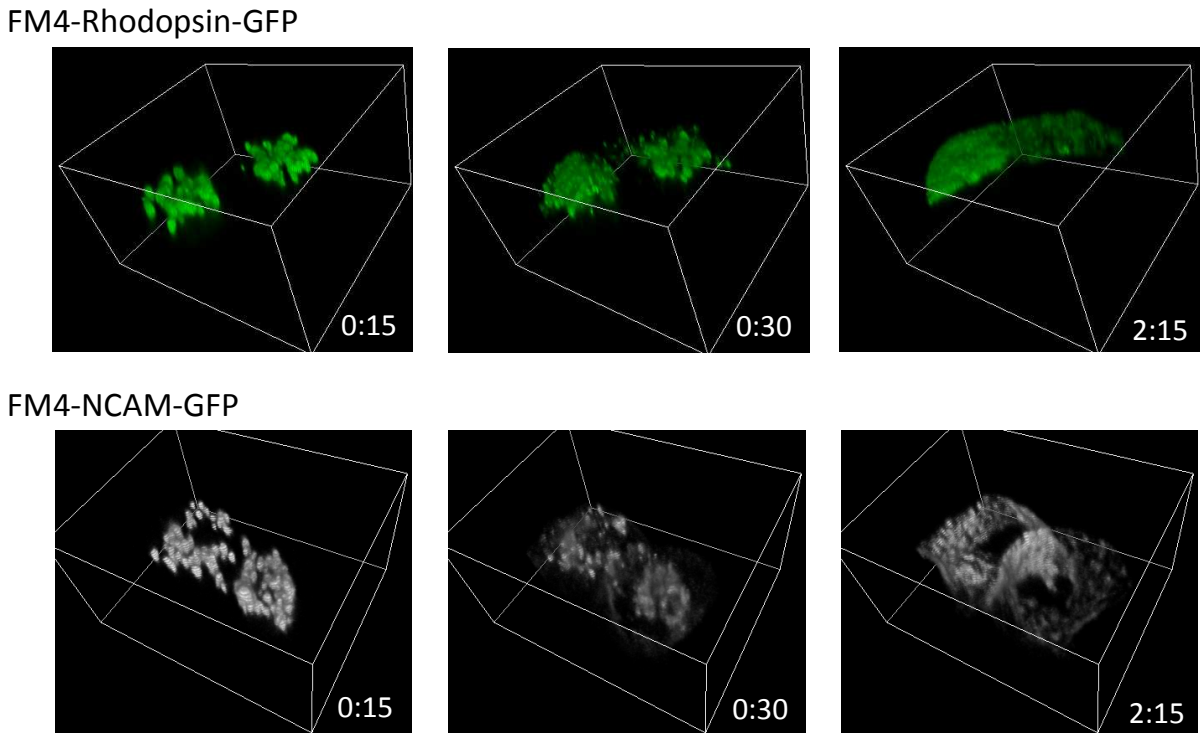

Figure 8. Targeting of FM4-constructs in polarized epithelial cells

The FM4-version of the apical membrane protein Rhodopsin, FM4-Rhodopsin-GFP, is targeted to the apical plasma membrane in polarized MDCK cells while the FM4-version of the basolateral membrane protein neural cell adhesion molecule (NCAM), FM4-NCAM-GFP, is targeted to the basolateral membrane. The figures show a 3D representation of the distribution of FM4-Rhodopsin-GFP (upper row) and FM4-NCAM-GFP (lower row) in polarized filter grown cells 15, 30 and 135 min after addition of AP21998.

Rhodopsin trafficking route to the plasma membrane

Golgi exit dynamics of FM4-Rhodopsin-GFP

A first startling observation was made in non-polarized MDCK cells stably expressing the Golgi marker sialyl transferase-RFP (ST-RFP). In these cells it can clearly be seen that FM4-Rhodopsin-GFP accumulates in an intracellular pericentriolar compartment before it translocates to the plasma membrane (Figure 9A) but after exit from the Golgi. The same observation can be made in polarized cells (Figure 9B), although the intermediate compartment is not as clearly separated from the ST-

RFP labeled Golgi and the apical plasma membrane because in polarized cells these compartments are much closer packed along the z-direction where also the resolution of the confocal microscope is lower as in x and y direction (Jaiswal 2009).
To further analyze and quantify the Golgi exit of FM4-Rhodopsin-GFP we developed a Matlab program that allows determining the amount of FM4-Rhodopsin-GFP co-localizing with ST-RFP over time. As co-localization parameter we chose an overlap coefficient (OL) which is defined as a Manders co-localization coefficient (Manders, Verbeek et al. 1993) according to:

$$OL = \Sigma_i G_{i,col} / \Sigma_j G_j \qquad (1)$$

In order to calculate OL, threshold values were defined for the green and the red channel. For the green channel FM4-Rhodopsin-GFP positive voxels were defined as voxels with an intensity value above the threshold (and analogous for the red channel); the intensity values for these j voxels are denoted as G_j in (1). Co-localizing voxels were defined as voxels having an intensity above the defined threshold values in both channels; the intensity values for these i voxels are denoted as $G_{i,col}$ in (1). We found that the time course of OL determined by this algorithm depended only weakly on the chosen threshold values if the values remained within a reasonable range that did not change the overall appearance of the images which was controlled by visual inspection.
As seen in Figure 9A and 9B the OL_{Golgi} coefficient measuring the amount of FM4-Rhodopsin-GFP at the Golgi is peaking around 20 – 30 min after addition of AP21998 and then declining as the Golgi empties. Please note that the time 0 min is defined as time of addition of AP21998, the actual live cell imaging starts at 15 min due to the time needed to transfer the cells to the microscope and set up the measurement.

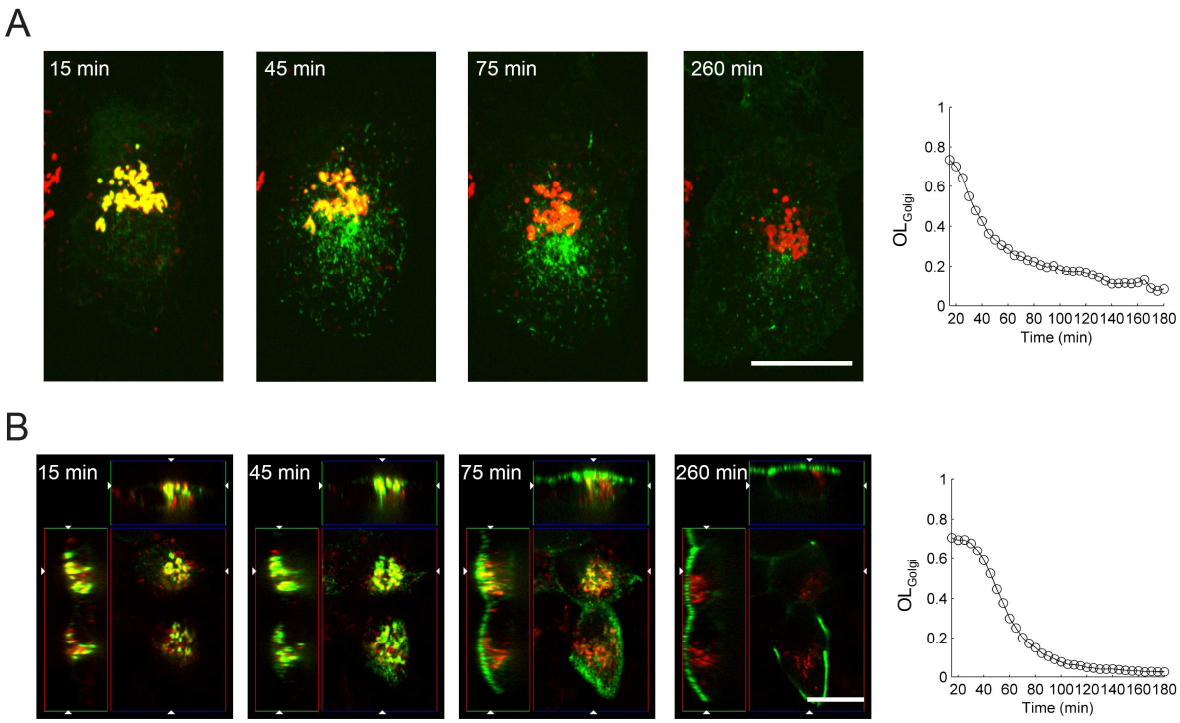

Figure 9. Exit of FM4-Rhodopsin-GFP from the Golgi

(A) The figure shows a time lapse of the release of FM4-Rhodopsin-GFP (green) in ST-RFP (red) expressing non-polarized MDCK cells. For every indicated time point a maximum intensity projection of the recorded z-stack is shown. For recording, non-polarized MDCK cells have been transfected with Lipofectamine 2000 for 5 h. Next cells were pre-incubated with cycloheximide for 1 h. For measurement the medium was changed to recording medium supplemented with 5 µM AP21998 and 100 µg/ml cycloheximide. The dish was transferred to the microscope and expressing cells were localized. At this time most of FM4-Rhodopsin-GFP localizes already to the Golgi as can be seen by the extensive co-localization. It is evident that Rhodopsin traverses a pericentriolar compartment before it is inserted into the plasma membrane. The scale bar corresponds to 20 µm. The graph on the right hand side displays the OL_{Golgi} coefficient measuring the amount of FM4-Rhodopsin-GFP co-localizing with the Golgi.

(B) The figure shows a time lapse of the release of FM4-Rhodopsin-GFP (green) in ST-RFP (red) expressing polarized MDCK cells. For every indicated time point a vertical xz- and yz-sections and a horizontal xy-section at the level of the tight junctions is shown. Recording was done in the same way as described in (A). Within approximately 90 min FM4-Rhodopsin-GFP empties gradually from the Golgi and is vectorially inserted into the apical plasma membrane. The scale bar corresponds to 20 µm. The graph on the right hand side displays the OL_{Golgi} coefficient measuring the amount of FM4-Rhodopsin-GFP co-localizing with the Golgi.

Passage of FM4-Rhodopsin-GFP through the Rab11-compartment

In order to determine the nature of the compartment that is traversed by FM4-Rhodopsin-GFP we looked at co-localization with compartment markers. A good candidate is Rab11, as it is found at the pericentriolar recycling compartment in non-polarized cells (Ullrich, Reinsch et al. 1996) and is also implicated in apical trafficking in polarized epithelial cells (Cresawn, Potter et al. 2007; Weisz and Rodriguez-Boulan 2009; Bryant, Datta et al. 2010) and has been shown to be implicated in Rhodopsin trafficking in Drosophila (Satoh, O'Tousa et al. 2005; Li, Satoh et al. 2007). As shown in Figure 10A, in non-polarized cells stably expressing a fluorescent version of Rab11, Rab11-mCherry, a clear co-localization with FM4-Rhodospin-GFP peaking at approximately 50-60 min after addition of AP21998 was observed. The same result was achieved if the co-localization of FM4-Rhodopsin-GFP with endogenous Rab11 was investigated by immunofluorescence in fixed cells (Figure 11), proving that the exogenously introduced Rab11-mCherry labeled indeed the endogenous Rab11-compartment. Also in polarized cells (Figure 10B) FM4-Rhodopsin-GFP can be seen co-localizing with the Rab11 compartment peaking at 50-60 min after the release. In order to exclude possible false interpretation of the co-localization signal between Rab11 and Rhodopsin, we looked as negative control at the basolateral protein NCAM (Le Gall, Powell et al. 1997) that is believed not to pass through a Rab11 compartment en route to the plasma membrane. As expected, during the whole time course no significant co-localization between Rab11-mCherry and the synchronized cohort of FM4-NCAM-GFP could be detected (Figure 12).

In summary this data suggests that Rhodopsin is traversing a Rab11-positive compartment en route to the plasma membrane in both non-polarized and polarized epithelial cells.

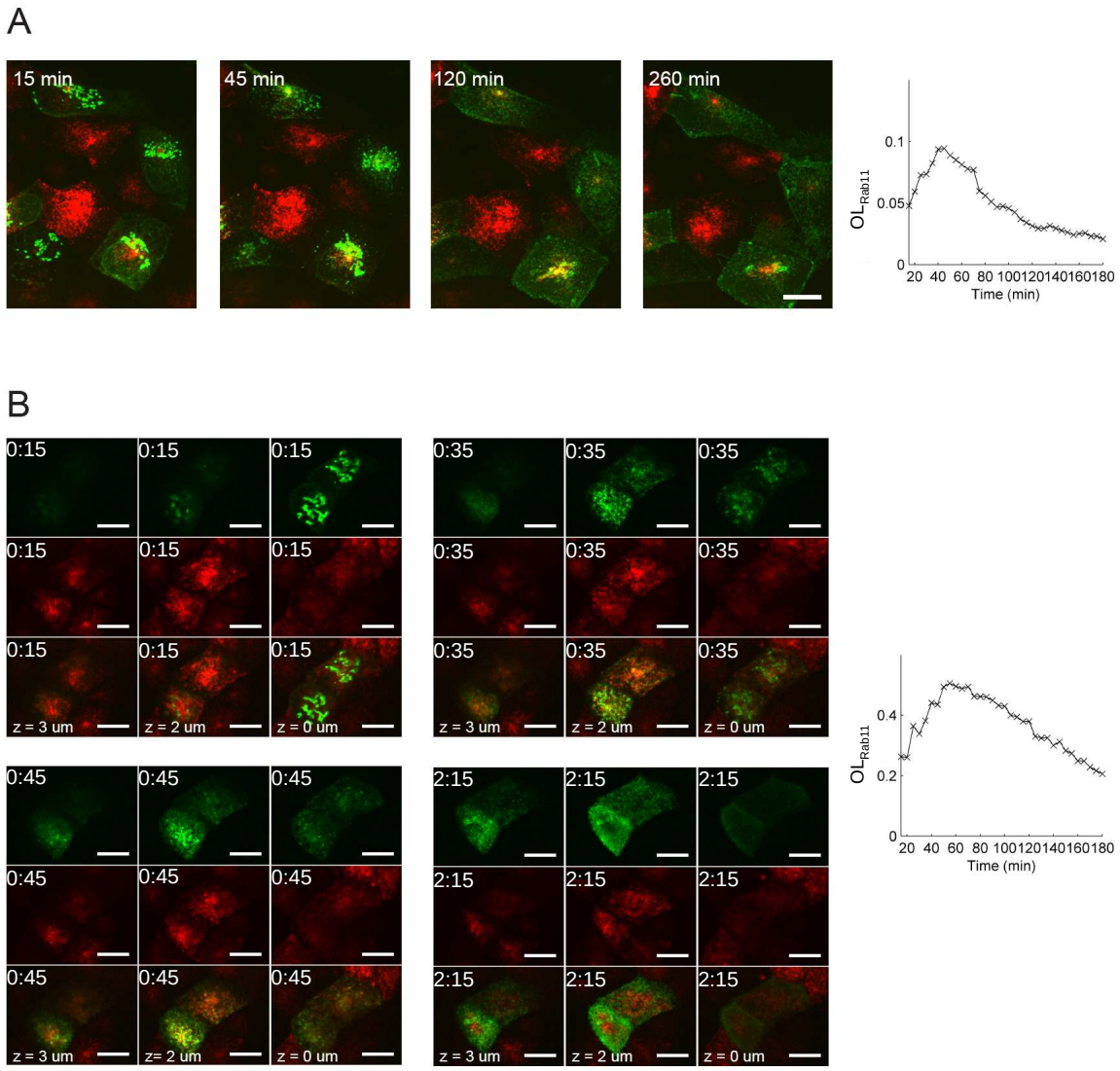

Figure 10. Rhodopsin is passing through a Rab11-compartment

(A) The figure shows a time lapse of the release of FM4-Rhodopsin-GFP (green) in Rab11-mCherry (red) expressing non-polar MDCK cells. For every indicated time point a maximum intensity projection of the recorded z-stack is shown. Rhodopsin is trafficked first to the pericentriolar, Rab11-positive compartment before it is inserted into the plasma membrane. The scale bar corresponds to 20 µm. (B) The figure shows a time lapse of the release of FM4-Rhodopsin-GFP (green) in Rab11-mCherry (red) expressing polarized MDCK cells. Three different z-planes per time point are displayed: one at the level of the apical plasma membrane (z = 3 µm), one at the Rab11-compartment (z = 2 µm) and one at the Golgi (z = 0 µm). Rhodopsin trafficked out from the Golgi is first co-localizing with the Rab11-compartment - peaking at approximately 50-60 min - and is subsequently inserted into the apical plasma membrane. The scale bars corresponds to 10 µm.

The graphs on the right hand side display the OL_{Rab11} coefficient measuring the amount of FM4-Rhodopsin-GFP co-localizing with Rab11-mCherry.

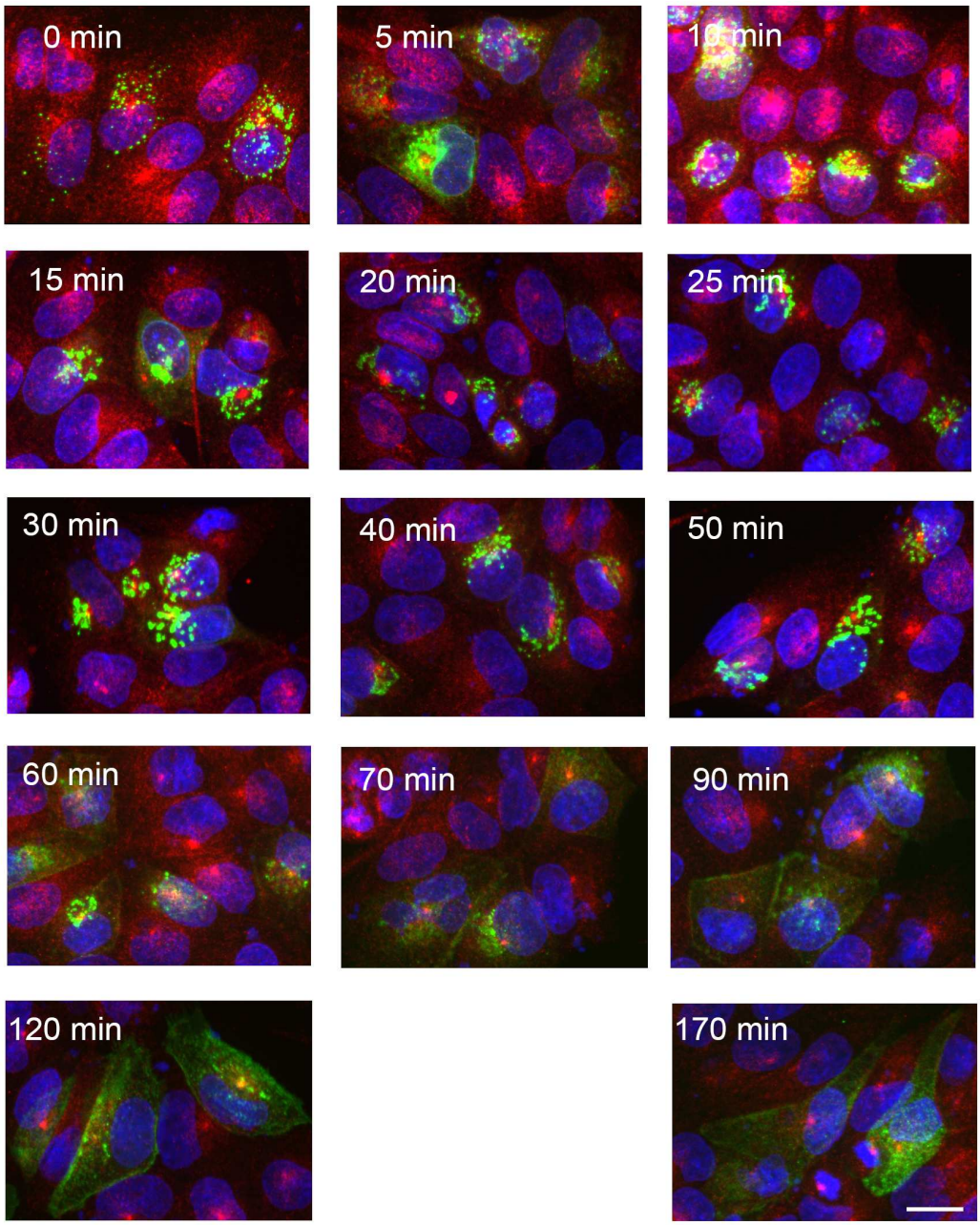

Figure 11. Rhodopsin is passing through the endogenous Rab11-compartment en route to the plasma membrane.

The Figure shows a similar experiment as Figure 10A, but here wt-MDCK cells are used. For every time point a maximum intensity projection of the recorded z-stack is shown. The cells were fixed at the indicated time points (time 0 min is the time for the addition of the release drug, time 15 min is the time when imaging would start at an live cell experiment) and immunostained for endogenous Rab11 (red) and nuclei (blue); FM4-Rhodopsin-GFP is shown in green. The scale bar corresponds to 20 µm.

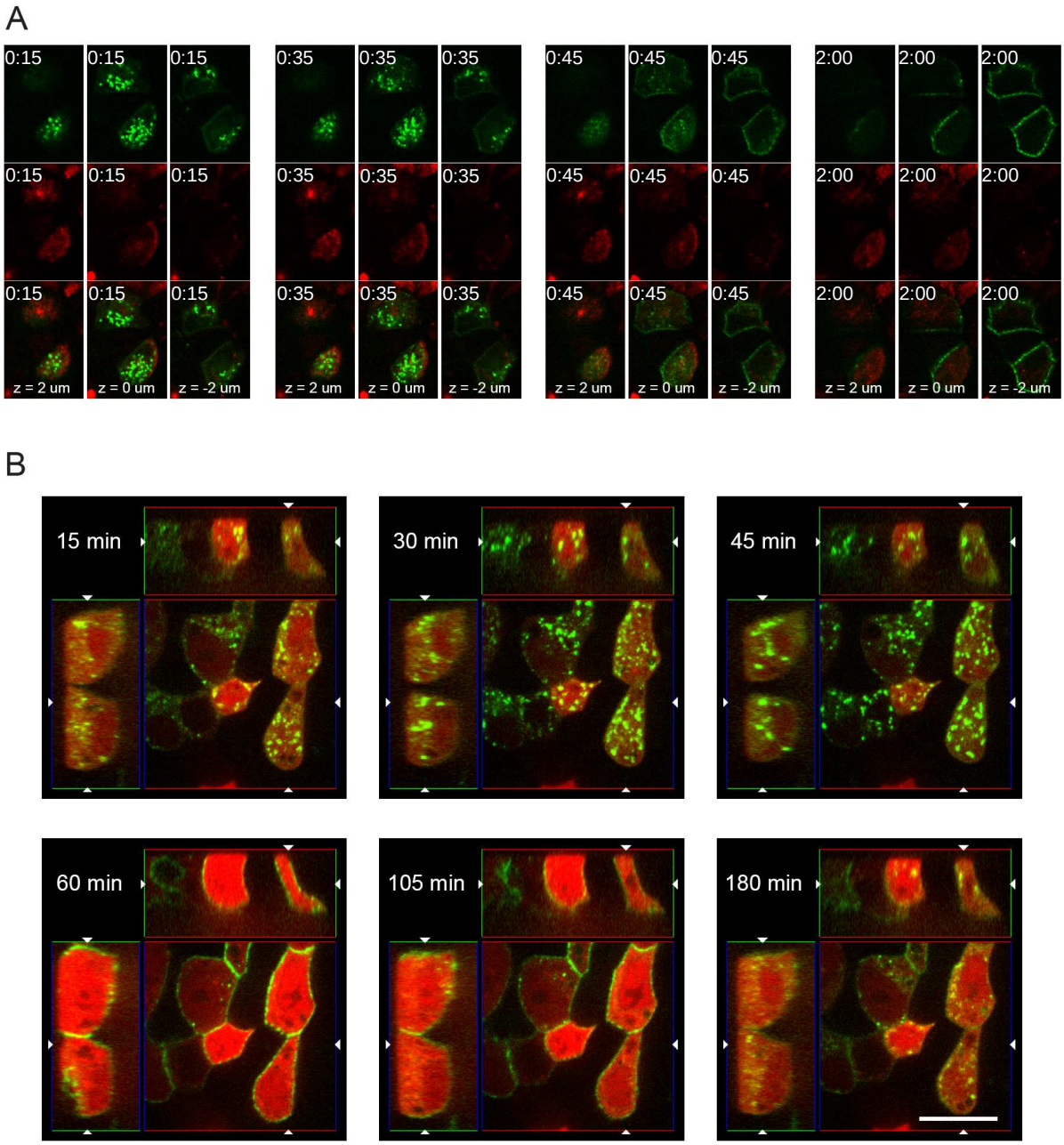

Figure 12. The basolateral protein NCAM is not traversing the Rab11-compartment en route to the plasma membrane.

(A) shows a time lapse of FM4-NCAM-GFP (green) released in polarized cells expressing Rab11-mCherry (red). Three different z-planes per time point are displayed: one at the level of the Rab11-compartment (z = 2 µm), one at the Golgi (z = 0 µm), one below the Golgi, where the lateral membrane is clearly visible (z = -2 µm). No co-localization between Rab11-mCherry and FM4-NCAM-GFP occurs during the whole time course.

(B) shows that Rab11-mCherry-DN (red) does not influence the basolateral trafficking of FM4-NCAM-GFP (green). For every indicated time point vertical xz- and yz-sections and a horizontal xy-section is shown. The scale bar corresponds to 20 µm.

To further control that FM4-Rhodopsin-GFP is passing through a Rab11 compartment and also to determine a functional role of Rab11 in the trafficking route we studied the effects of a dominant negative GDP-locked form of Rab11 tagged with mCherry, Rab11-mCherry-S25N (Wang, Kumar et al. 2000) on FM4-Rhodopsin-GFP trafficking. Rab11-mCherry-S25N is permanently in a non-membrane bound state and therefore homogenously distributed in the cytosol ((Chu, Ge et al. 2009), see also Figure 13). Surprisingly, in non-polarized cells expressing Rab11-mCherry-S25N FM4-Rhodopsin-GFP reached the plasma membrane without significant disturbance (Figure 13A). In polarized cells the situation looked entirely different (Figure 13B). Here Rab11-mCherry-S25N induces intracellular retention of FM4-Rhodopsin-GFP and also a re-routing to the basolateral membrane.

The applied co-transfection strategy of Rab11-mCherry-S25N and FM4-Rhodopsin-GFP ensured that the cells express a sufficient amount of dominant negative Rab11 while FM4-Rhodopsin-GFP is still retained at the ER. Therefore the effects of a malfunctioned Rab11-compartment can be more precisely determined as if non-regulateable Rhodopsin-GFP would be used because at early times, when Rab11-mCherry-S25N was not yet able to take control of the Rab11 compartment, Rhodopsin-GFP would have been already trafficked to the compartment. However, even simple co-expression of Rhodopsin-GFP and Rab11-S25N for 24h results in qualitatively analog effects (personal communication of Ching-Hwa Sung, Dyson Vision Research Institute, Weill Cornell Medical College).

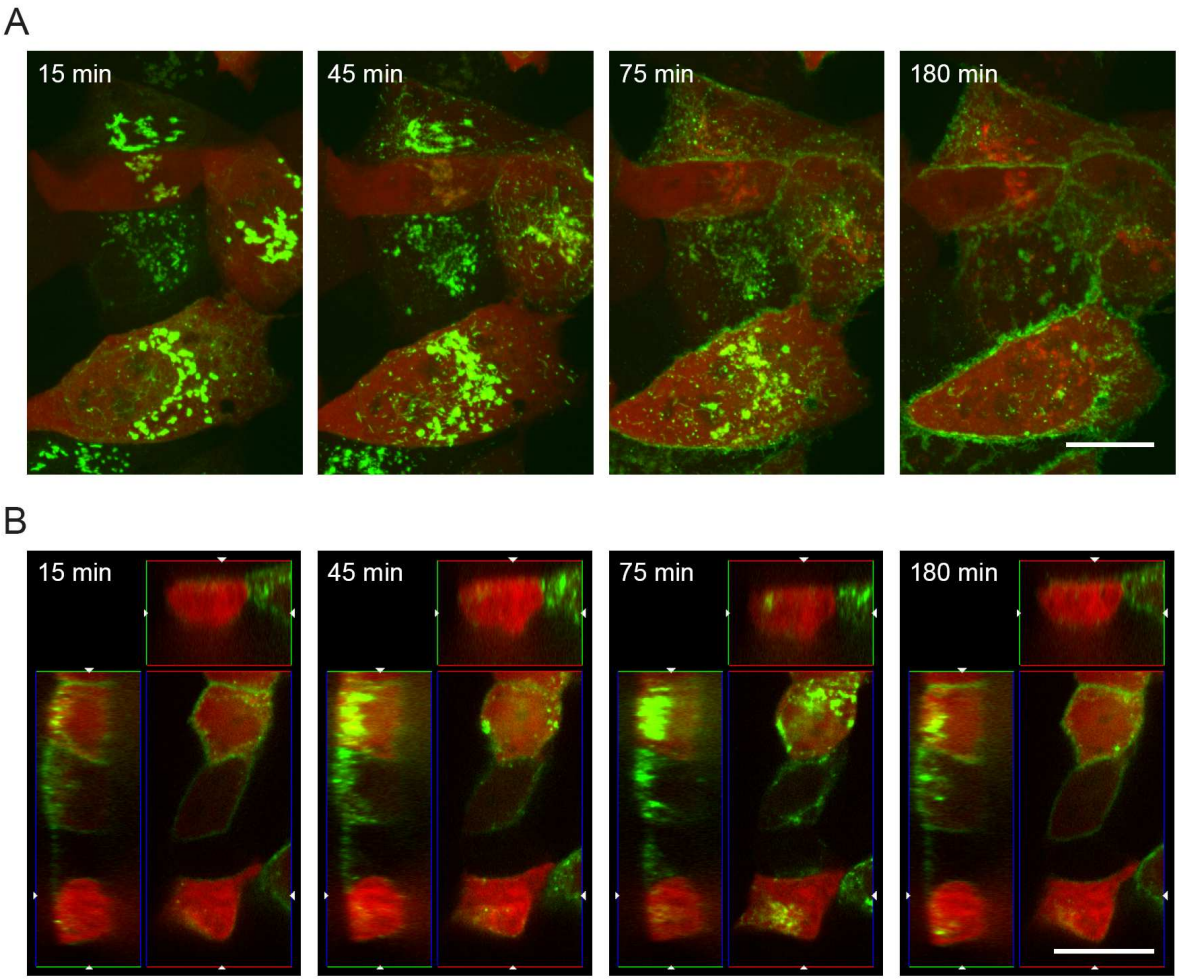

Figure 13. Dominant negative Rab11 inhibits Rhodopsin transport to the apical plasma membrane.

(A) shows a time lapse of the release of FM4-Rhodopsin-GFP (green) in dominant negative Rab11-mCherry (Rab11-mCherry-S25N, red) expressing non-polarized cells. For every indicated time point a maximum intensity projection of the recorded z-stack is shown. Here, no significant inhibition of Rhodopsin transport to the plasma membrane is evident. The scale bar corresponds to 20 µm.

(B) shows the same experiment as in (A) but for polarized MDCK cells. For every indicated time point vertical xz- and yz-sections and a horizontal xy-section is shown. It can be seen that in Rab11-mCherry-DN expressing cells Rhodopsin is not tranported to the apical membrane but is instead retained intracellularly and also redirected to the basolateral membrane. The scale bar corresponds to 20 µm.

An additional control that the observed effects of dominant negative Rab11 are specific for this GTPase is that dominant negative Rab5, a GTPase involved in the formation of early endosomes (Zerial and McBride 2001; Maxfield and McGraw 2004), does not interfere with FM4-Rhodopsin-GFP apical targeting in polarized cells (Figure 14).

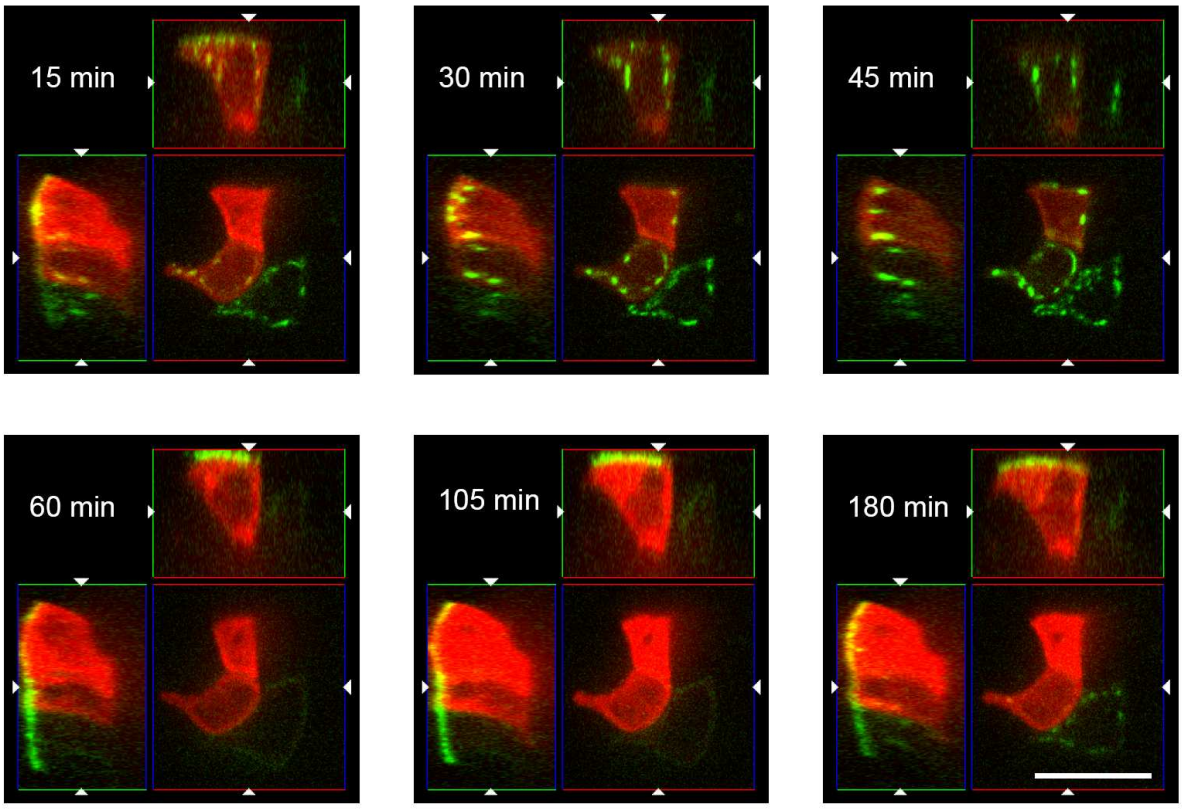

Figure 14. Dominant negative Rab5 does not interfere with apical trafficking of FM4-Rhodopsin-GFP.

The figure shows that Rab5-mCherry-DN (red) does not influence apical trafficking of FM4-Rhodopsin-GFP (green). For every indicated time point vertical xz- and yz-sections and a horizontal xy-section is shown. The scale bar corresponds to 20 µm.

From these results it is clear that Rab11 is required in the apical trafficking route of Rhodopsin in polarized MDCK cells, after exit from the TGN. However, at this stage the detailed mechanistic or regulatory role of Rab11 along the remaining trafficking route remains to be established. Several possibilities are emerging: The role of Rab11 could be restricted to the so-called Rab11 compartment and relies in regulating traffic towards and out of this compartment. Alternatively, Rab11 could be

present at vesicles till fusion with the plasma membrane occurs and therefore also play a regulatory role in the fusion process.

An interesting finding in this context is that, as shown in Figure 15, Rhodopsin-GFP-positive vesicles undergoing fusion with the plasma membrane in non-polarized MDCK cells also carry Rab11-mCherry. Closer inspection of the kinetics of both proteins during the fusion process reveals that Rab11 leaves the fusion site much earlier than Rhodopsin. While a clear Rhodopsin signal continues to be present till 2700 ms, the Rab11 signal is vanishing after approximately 600 ms. This clearly hints to a regulatory role of Rab11 at the vesicle fusion process.

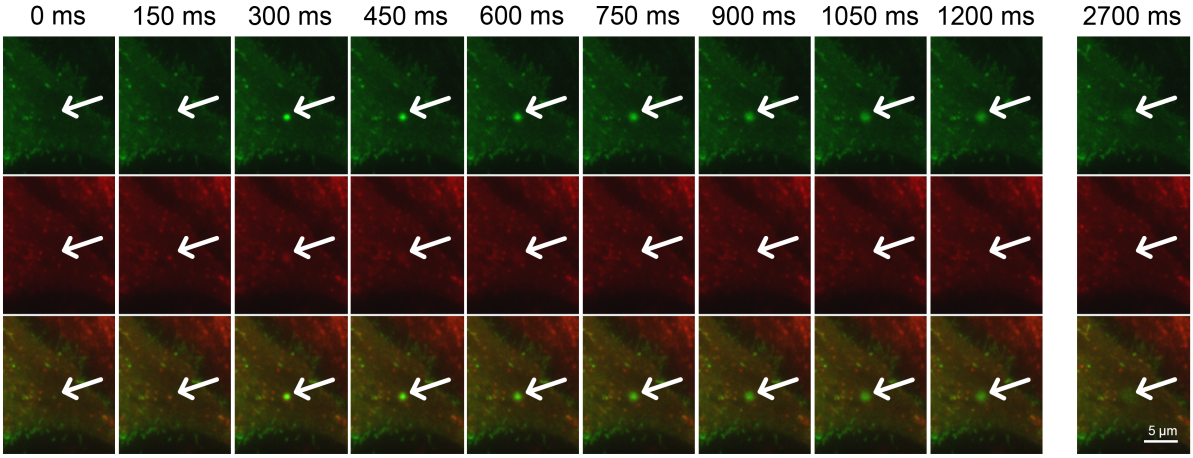

Figure 15: Rhodopsin-bearing vesicles fusing with the plasma membrane also carry Rab11

The Figure shows a dual-color time lapse of Rhodopsin-GFP (green) and Rab11-mCherry (red) of a vesicle fusion event at the apical membrane as recorded by TIRF microscopy. For recording, non-polarized MDCK cells were transfected with Rhodopsin-GFP and Rab11-mCherry. Next the cells were subjected to Golgi exit temperature block for 2 h. The temperature block was released by reheating to 37°C at the microscope. The white arrow points to the fusion event that starts between 150 ms and 300 ms. Note that Rab11 is removed from the site of fusion much faster than Rhodopsin-GFP. The scale bar corresponds to 5 µm.

Apical TIRF recording of Rhodopsin vesicle fusion events

For apical TIRF measurements the two versions of the biochip for apical TIRF microscopy (see Figures 4 and 5) have been extensively tested. The tests revealed

that the version 2 of the chip is much easier to handle and was therefore used for the further experiments. Most of the detected vesicle fusion events are similar to those that have been reported at the basal membrane (vesicles 2 and 3 in Figure 16; (Schmoranzer, Goulian et al. 2000; Toomre, Steyer et al. 2000)). But also some interesting new variants of vesicle fusion behavior have been observed that do not occur at the basal membrane. Occasionally, non-radial spreading of the vesicular content after fusion was observed (vesicle 1 in Figure 16). For interpretation it has to be considered that the apical membrane is decorated with microvilli in contrast to the flat basal membrane (Rodriguez-Boulan, Kreitzer et al. 2005). A possible explanation for the non-radial spreading would be that vesicle 1 was fusing at the base of – in this case three – microvilli and the content of the vesicle diffused into and along the microvilli after fusion. Apical TIRF microscopy allowed also to monitor the topographic distribution of vesicle fusion sites at the apical membrane. As shown in Figure 17 an equal distribution of fusion sites all over the apical membrane was observed.

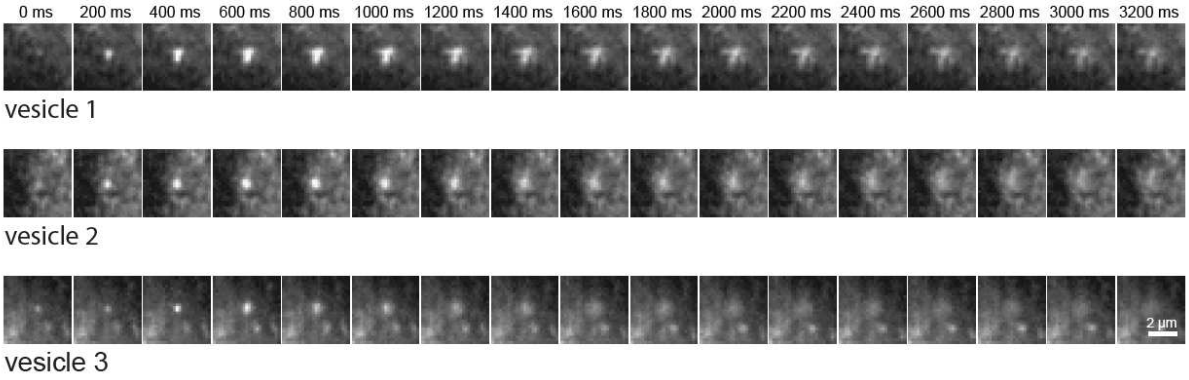

Figure 16: Apical TIRF is capable of visualizing individual fusion events of Rhodopsin-GFP bearing vesicles

A variety of different behaviors can be seen for Rhodopsin-GFP bearing vesicles fusing with the apical plasma membrane. The Figure shows the time lapse of different types of Rhodopsin-GFP bearing vesicle fusion events as recorded by apical TIRF microscopy after the release of a Golgi exit temperature block. For recording, polarized MDCK cells were transfected with Rhodopsin-GFP and subjected to a Golgi exit temperature block for 2 h. The temperature block was released by reheating to 37°C at the microscope. While vesicle 1 shows an asymmetric, non-radial spreading of its content after fusion, probably along three microvilli, vesicle fusion events 2 and 3 are symmetrical. The scale bar corresponds to 2 µm.

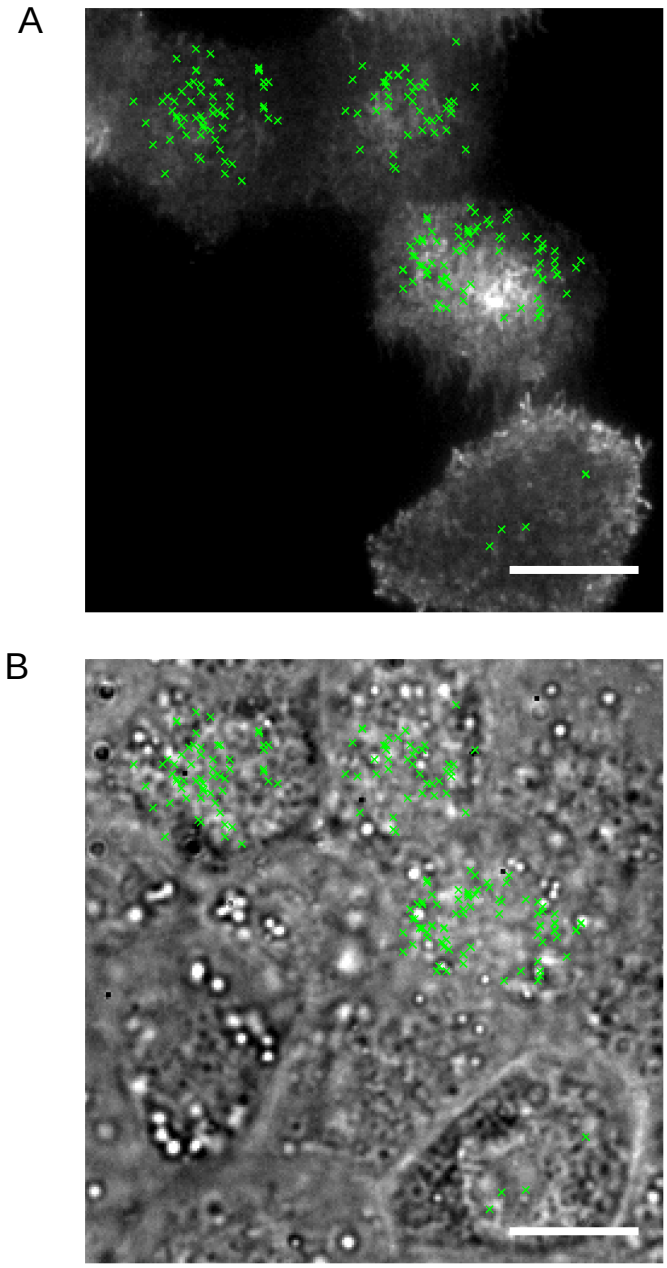

Figure 17. Distribution of fusion events of Rhodopsin-bearing vesicles at the apical membrane of polarized MDCK cells.

(A) The image shows an apical TIRF image after the release of a Golgi temperature block of Rhodopsin-GFP. Overlayed are the sites of individual vesicle fusion events during a time period of twelve minutes (marked with green x). The four cells that are expressing Rhodopsin-GFP exhibit an equal distribution of vesicle fusion sites over the entire apical membrane. The scale bar corresponds to 10 µm.

(B) Shows a white light image from the same cells as in (A). Overlayed are the sites of individual vesicle fusion events during a time period of twelve minutes (marked with green x). The scale bar corresponds to 10 µm.

Trafficking route of CAR-Y318A

In this chapter several experiments using the coxsackievirus and adenovirus receptor (CAR) are presented that support the findings for the role of Rab11 in apical membrane trafficking from the previous chapter.

The CAR protein

CAR is the receptor that mediates the infection for group B coxsackieviruses and most adenovirus serotypes (Diaz, Gravotta et al. 2009). It is a component of the epithelial junction complex and also found all over the basolateral plasma membrane in polarized MDCK cells. CAR is of interest not only from a pathological perspective but also as key player for gene therapies that are based on adenoviruses.

Figure 18A illustrates the protein domains and motifs present in the CAR protein. The sequence YNQV starting at position 318 of CAR comprises a basolateral sorting motif (YXXΦ; X stands for any amino acid and Φ stands for a hydrophic residue) (Bonifacino and Traub 2003; Gonzalez and Rodriguez-Boulan 2009). As can be seen in Figure 18B CAR-wt is targeted to the apical plasma, while CAR-Y318A, which has a mutated non-functional sorting motif, is targeted to the apical cell pole.

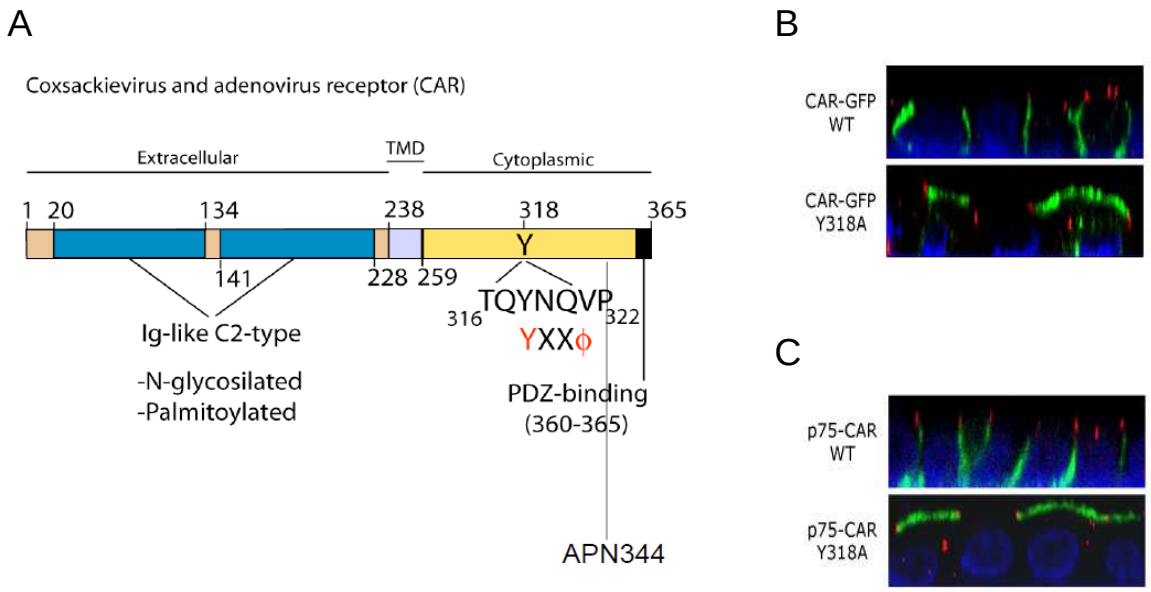

Figure 18. Properties of the CAR protein (images courtesy of Jose Maria Carvajal-Gonzalez (Dyson Vision Research Institute, Weill Cornell Medical College)

(A) shows the domains present at CAR. The tyrosine at position 318 is part of a basolateral targeting signal.

(B) wt-CAR-GFP stably transfected to MDCK cells localizes to the basolateral plasma membrane while the mutant CAR-Y318A localizes to the plasma membrane. The tight junction protein ZO1 is counterstained in red.

(C) The cytoplasmic tail of CAR fused to the apical plasma membrane protein p75-GFP re-routes the resulting protein (p75-CAR-wt) to the basolateral membrane while p75-CAR-Y318A remains at the apical membrane. The tight junction protein ZO1 is counterstained in red.

During the research stay at the Rodriguez-Boulan lab regulate-able FM4-versions of CAR-wt-GFP and CAR-Y318A-GFP have been produced. Figure 19 shows that these versions are targeted to the basolateral (FM4-CAR-wt-GFP) and the apical plasma membrane (FM4-CAR-Y318A-GFP) as expected.

FM4-CAR-wt-GFP

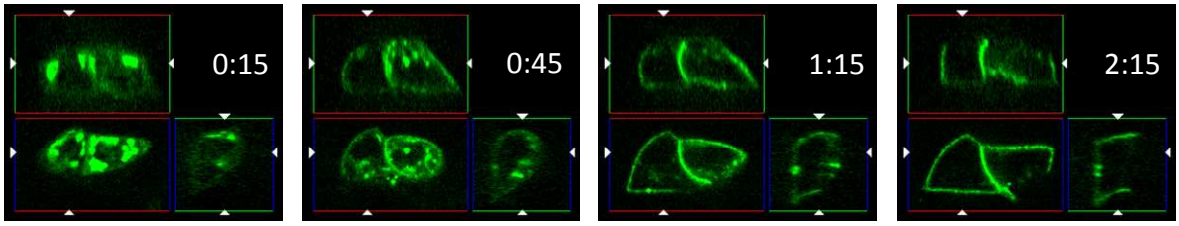

FM4-CAR-Y318A-GFP

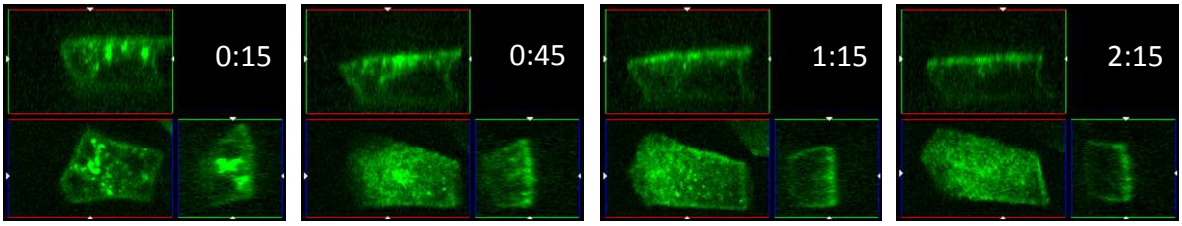

Figure 19. Properties of the FM4-versions of the CAR protein

Top row: FM4-CAR-GFP-wt is targeted to the basolateral membrane after being released form the ER upon addition of AP21998.

Bottom row: FM4-CAR-Y318A-GFP is targeted to the apical membrane after being released form the ER upon addition of AP21998.

The role of Rab11 for apical CAR-Y318A trafficking

As the mutant CAR-Y318A is re-routed to the apical cell pole, the question is arising if it is using a Rab11-dependent apical route. As shown in Figure 20 this is indeed the case, because co-expression of the dominant negative Rab11-S25N-mCherry induces intracellular retention and also re-routing to the basolateral plasma membrane. In contrast, targeting of CAR-wt to the basolateral plasma membrane is not influenced by Rab11-S25N-mCherry expression (Figure 21).

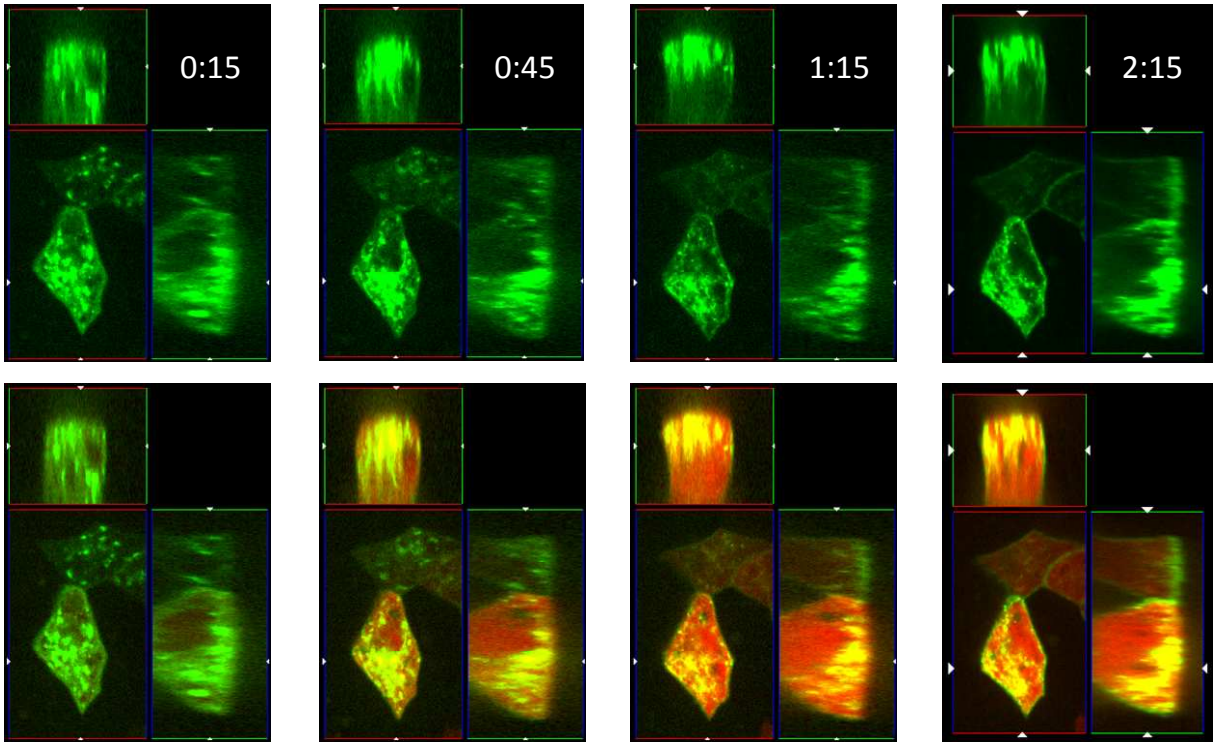

Figure 20. Rab11-mCherry-S25N causes intracellular retention and basolateral re-routing of FM4-CAR-Y318A-GFP

The figure shows a time lapse of the release of FM4-CAR-Y318A-GFP (green) in dominant negative Rab11-mCherry (Rab11-mCherry-S25N, red) expressing polarized MDCK cells. For every indicated time point vertical xz- and yz-sections and a horizontal xy-section is shown (First row: FM4-CAR-Y318A-GFP only; second row: overlay).

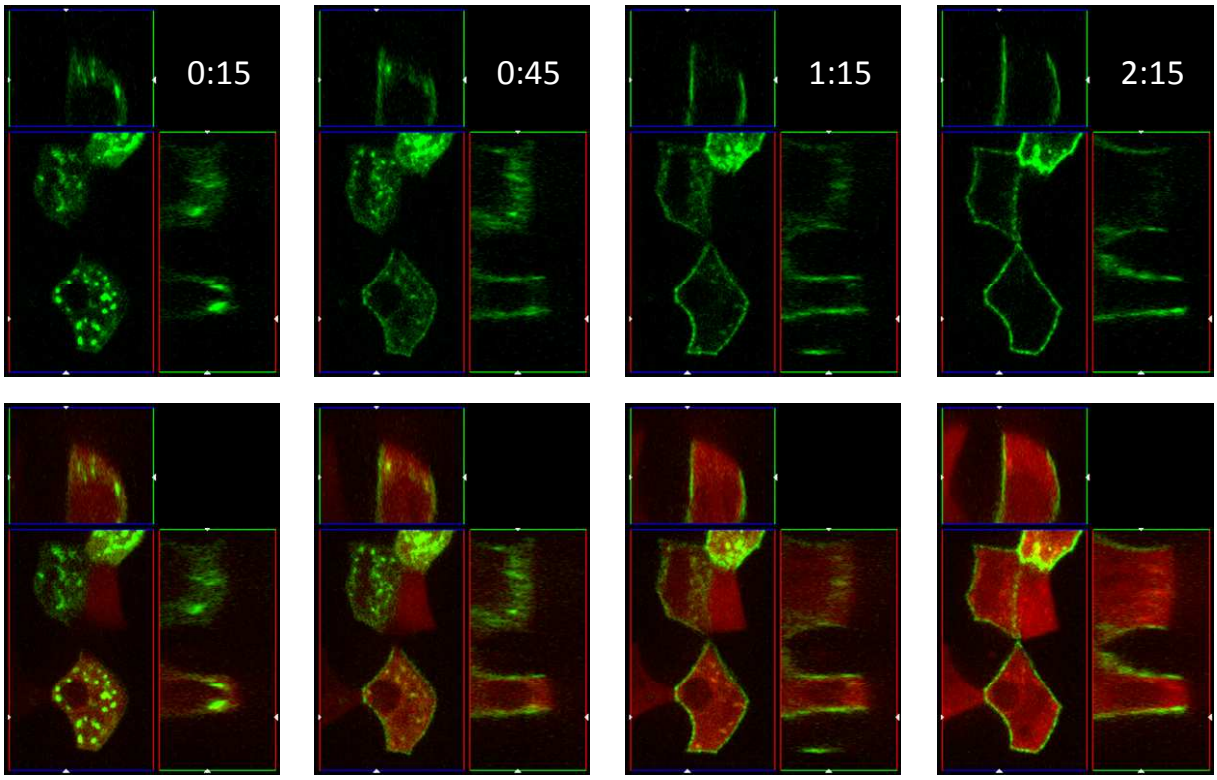

Figure 21. Rab11-mCherry-S25N does not interfere with basolateral targeting of FM4-CAR-GFP-wt.

The figure shows a time lapse of the release of FM4-CAR-GFP-wt (green) in dominant negative Rab11-mCherry (Rab11-mCherry-S25N, red) expressing polarized MDCK cells. For every indicated time point vertical xz- and yz-sections and a horizontal xy-section is shown (First row: FM4-CAR-GFP-wt only; second row: overlay).

Discussion

Role of the Rab11 compartment in polarized cells

An emerging concept in intracellular trafficking is that almost all plasma membrane proteins traverse intracellular endocytic compartments after exit from the trans-Golgi network but before arrival at the plasma membrane. The reasons for this are not yet well understood but may include sorting occurring at this compartments (Mellman and Nelson 2008; Weisz and Rodriguez-Boulan 2009), compartments serving as storage pools (Nedvetsky, Stefan et al. 2007) or even signaling taking place via proteins present at this intermediate localization during development of polarity (Bryant, Datta et al. 2010). Studying these processes is difficult because knocking down key components of relevant compartments interferes typically with establishment of polarity (Bryant, Datta et al. 2010). Further, in order to clearly visualize co-localization of a plasma membrane protein of interest with a compartment marker a synchronized delivery of a labeled cohort of the protein of interest is required. Therefore we combined immediate functional knockdown of Rab11 by expression of a dominant negative variant of Rab11 in already fully polarized cells with a regulated trafficking system.

The obtained data shows that Rhodopsin is passing through the Rab11 compartment in non-polarized cells. In non-polarized cells no sorting decision has to be made, this can explain why dominant negative Rab11-mCherry-S25N does not interfere with plasma membrane traffic under these conditions. In polarized cells the Rab11 compartment acquires a different role. It has been established that many apical membrane proteins including gp135 (Bryant, Datta et al. 2010) and endolyn (Cresawn, Potter et al. 2007) pass through the Rab11 compartment en route to the plasma membrane. Also one basolateral protein, E-Cadherin, has been identified to traverse the Rab11 compartment (Lock and Stow 2005; Desclozeaux, Venturato et al. 2008). This implicates that an active sorting decision has to be made at this compartment. This is supported by our finding that in polarized cells active and functional Rab11 is necessary for apical targeting of both Rhodopsin and CAR-Y318A as dominant negative Rab11-mCherry-S25N redirects both proteins to the basolateral membrane and induces partial intracellular retention. Further it has been

found in (Desclozeaux, Venturato et al. 2008) that dominant negative Rab11-mCherry-S25N redirects E-cadherin to the apical cell pole.

Another interesting observation is that Rab11 is present at Rhodopsin-bearing vesicles that fuse with the plasma membrane in non-polarized cells and is also removed quickly from the site of fusion. Although this hints to a regulatory role of Rab11 in the fusion process, Rab11 function appears not to be a necessary prerequisite for membrane insertion of Rhodopsin trafficked along the biosynthetic route in non-polarized cells as Rab11-mCherry-S25N expression does not prevent membrane insertion in this case. Further dual color TIRF experiments utilizing the apical TIRF biochip at the Center for Advanced Bioanalysis in Linz are ongoing in order to define the role of Rab11 in the vesicle fusion at the apical membrane of polarized cells.

Apical vesicle fusion characteristics

The obtained data using single color apical TIRF microscopy measurements provided interesting insights into the apical fusion process of Rhodopsin-bearing vesicles. The apical membrane can not be seen as one homogenous compartment because part of the apical membrane is the primary cilium that shows a different protein composition (Weisz and Rodriguez-Boulan 2009) that is maintained by a diffusion barrier at the base of the cilium (Hu, Milenkovic et al. 2010). Little is known about the machinery that mediates sorting and trafficking to the primary cilium (Weisz and Rodriguez-Boulan 2009). While Rhodopsin is targeted to the outer segment of photoreceptor cells (Sung and Chuang 2010), an organelle that is reminiscent to the primary cilium, we could not detect Rhodopsin in the primary cilium of polarized MDCK cells. Instead, Rhodopsin and also the fusion sites of Rhodopsin-bearing vesicles are distributed equally all over the apical membrane. Further, occasionally detected non-radial diffusive spreading of the vesicular content after fusion suggests that apical vesicle fusion occurs at the base of microvilli.

Summary and Outlook

During the research stay a regulated trafficking system has been developed that allowed to study apical trafficking mechanisms of Rhodopsin in MDCK cells, a model system for polarized epithelial cells. Using this system we showed that functional Rab11 is necessary for biosynthetic Rhodopsin apical membrane trafficking in polarized cells while in non-polarized cells Rhodopsin membrane insertion did not depend on Rab11 activity. We could further show that the apical targeting of the mutant CAR-Y318A depends on Rab11 function while basolateral targeting of CAR-wt did not depend on Rab11. These results confirm the requirement for Rab11 in specific apical trafficking routes and suggest the new concept that an active sorting decision can be made at the subapical Rab11 compartment. In addition, by utilizing a PDMS-based biochip that enables performing TIRF microscopy at the apical plasma membrane we showed for the first time that vesicle fusion sites are scattered all over the apical membrane.

Taken together, the regulated trafficking system and the apical TIRF biochip are powerful tools that allow performing novel experiments to study the entire apical membrane trafficking route from the ER to the plasma membrane in unprecedented resolution and dynamics. In future we will apply the developed strategies for other proteins that are expected to take different routes to the apical membrane than Rhodopsin in order to further delete some white spots on the map of apical membrane trafficking.

Materials and Methods

All reagents were purchased from Sigma Aldrich unless stated otherwise.

Cells culture and creation of stable cell lines

Madin-Darby canine kidney strain II (MDCK II) cells were maintained in Dulbecco's modified Eagle's medium (DMEM, Invitrogen) supplemented with 5% fetal bovine serum at 37°C and 5% CO_2 and passaged by trypsinization. For creation of cell lines stably expressing Rab11-mCherry, MDCK II cells were transfected by electroporation (AMAXA) with the appropriate plasmid encoding the protein of interest and also the neomycin resistance gene. After 24h the cells were selected with 1 mg/ml G418 and clones showing a high expression of the protein of interest were selected and tested for correct development of polarization. The MDCK cell line stably expressing ST-RFP has been described in (Salvarezza, Deborde et al. 2009).

Microscopy system at the Rodriguez-Boulan lab

In order to be able to image intracellular membrane trafficking in polarized epithelial cells a high speed confocal microscope is necessary. Particularly spinning disc confocal microscopy combines high recording speed with the enhanced resolution of a confocal microscope. During the research stay a microscopy system based on a AxioObserver Z1 inverted microscope (Zeiss) was established at the Rodriguez-Boulan laboratory. The system was equipped with a CSU-X1 spinning disc unit (Yokogawa) and an ORCA R2 CCD camera (Hamamatsu). TIRF excitation was made possible by a Laser TIRF 3 slider (Zeiss), detection of the fluorescence signal of the TIRF channel was done with an EVOLVE EMCCD camera (Photometrics). Figure 22 shows a photograph of the microscopy system.

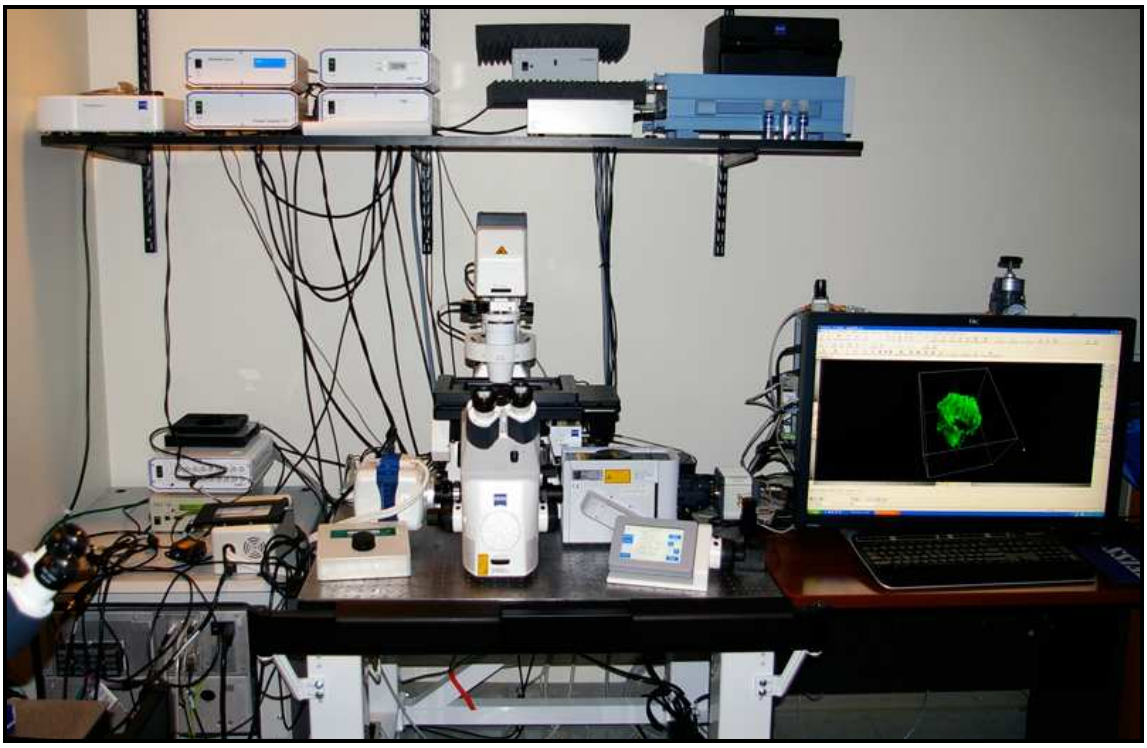

Figure 22. Microscopy system at the Rodriguez-Boulan laboratory equipped with a spinning disc unit and a Laser TIRF 3 slider.

Plasmids

pFM4-Rhodopsin-GFP was made in a two-step process. First, the human growth hormone signal sequence followed by four FM domains and a furin cleavage site was PCR amplified from the plasmid pC4S1-FM4-FCS-hGH (ARIAD) with the primer pair
5'-GACTGCTAGCGCCACCATGGCTACAGGCTCCCGGAC-3' and
5'-CGTAAGATCTGATCTCTTCTGACGGTTTCTAGC-3',
which introduces a BmtI restriction site at the 5' end and a BglII restriction site at the 3' end and then cloned into peGFP-N1 (Clontech) resulting in the plasmid pFM4-GFP. Second, Rhodopsin, tagged with GFP on its C-terminus and followed by a repeat of the last 8 residues of Rhodopsin, was PCR amplified from a plasmid described in (Yeh, Peretti et al. 2006) with the primer pair
5'-GACTAAGCTTATGAATGGCACAGAAGGCCC-3' and
5'-CGTAGCGGCCGCCTTAGGCCGGGGCCACCTG-3',
which introduces a HindIII restriction site at the 5' end and a NotI restriction site at the 3' end and then cloned into pFM4-GFP resulting in the plasmid pFM4-Rhodopsin-GFP.

pFM4-NCAM-GFP was made by the same strategy. NCAM-GFP was amplified from a plasmid described in (Deborde, Perret et al. 2008) using the primer pair
5'-GACTGGTACCACTACAAGTGGATATTGTTCC-3' and
5'-CGTAGGATCCCATGCTTTGCTCTCATTCTCA-3',
which introduces a KpnI restriction site at the 5' end and a BamHI restriction site at the 3' end and then cloned into pFM4-GFP resulting in the plasmid pFM4-NCAM-GFP.
The plasmids pFM4-CAR-GFP and pFM4-CAR-Y318A-GFP were a gift from Jose Maria Carvajal-Gonzalez (Dyson Vision Research Institute, Weill Cornell Medical College).
Rab11-mCherry was made from a plasmid encoding human Rab11a tagged at its N-terminus with GFP (gift from Ching-Hwa Sung, Dyson Vision Research Institute, Weill Cornell Medical College) by swapping the GFP for mCherry using the restriction enzymes AgeI and BsrgI. Rab11-mCherry DN was made from a plasmid encoding Rab11-S25N-GFP (gift from Ching-Hwa Sung, Dyson Vision Research Institute, Weill Cornell Medical College) by the same strategy.

Live cell confocal imaging of nonpolar cells

MDCK cells stably expressing ST-RFP or Rab11-mCherry were seeded on chambered cover glasses (Nunc, Labtek) at a density of 20.000 cells/cm2 and allowed to attach over night. Next morning the cells were transfected with FM4-Rhodopsin-GFP using Lipofectamine 2000 (Invitrogen) for 5-6h according to the instructions of the manufacturer. Cells were then incubated with 100 µg/µl cycloheximide for 1h. For measurement the medium was changed to recording medium (Hank's buffered salt solution (HBSS; Invitrogen) supplemented with 4.5 g/l glucose and 1 % FBS) supplemented with 100 µg/µl cycloheximide and 5µg/µl AP21998 (ARIAD). Imaging was done on a spinning disc confocal microscope using a 40x N.A. 1.4 objective (Zeiss), an additional 1.6x Optovar magnification and a sample holder maintained at 37°C.

Live cell confocal imaging of polarized cells

MDCK cells stably expressing ST-RFP or Rab11-mCherry were seeded on transwell filters with 0.4 µm pore size (Corning) at density of 300.000 cells/cm2 and allowed to

polarize for four days. On the day of measurement cells were transfected with FM4-Rhodopsin-GFP from the apical side only using Lipofectamine 2000 (Invitrogen) for 5-6h according to the instructions of the manufacturer, but applying the double amounts as indicated. Next, cells were incubated with 100 µg/µl cycloheximide for 1h. For measurement, the medium was changed to recording medium supplemented with 100 µg/µl cycloheximide and 5µg/µl AP21998 (ARIAD). The filter was cut out with a scalpel and placed with the cells pointing downwards to a glass cover slip. A cloning cylinder was placed on top of the filter in order to stabilize the cell layer in a position within the working distance of the objective. The actual measurement was done on a spinning disc confocal microscope using a 40x N.A. 1.4 objective (Zeiss), an additional 1.6x Optovar magnification and a sample holder maintained at 37°C.

Live cell experiments with Rab11-mCherry DN

Wt-MDCK cells were cotransfected with Rab11-mCherry DN and FM4-Rhodopsin for 5-6h. Cells were then washed and allowed to express the proteins for further 2h. Next, cells were incubated with 100 µg/µl cycloheximide for 1h. The actual measurement of Rhodopsin trafficking in these cells was done as described before.

Recording of apical vesicle fusion events

Four days old MDCK II monolayers grown on apical TIRF biochips were transfected for 6 h with Rhodopsin-GFP using Lipofectamine 2000. After washing, a 20 ℃ Golgi exit block was applied for 2 h to accumulate Rhodopsin-GFP in the Golgi. Prior to measurements the medium was replaced by recording medium. Chips were transferred to the microscope and placed upside-down on glass cover slips and re-heating to 37 ℃ was started on a heat-able microsc ope stage. To prevent adhesion of the apical membrane to the glass surface, the glass cover slips were coated prior to usage with bovine serum albumin (BSA) by incubation with a 5 % BSA solution for 30 min followed by rinsing with deionized water. During the experiment the focal plane was kept constant with a focus stabilization system. For recording apical membranes were approached to the glass cover slip by adjusting the pressure in the actuator channels and pre-existing Rhodopsin-GFP membrane signal in the evanescent wave region was removed by bleaching. Approximately 30 min after

reheating to 37℃ vesicles fusing with the apical membrane were observed using a 100x NA 1.46 apochromatic TIRF objective (Zeiss).

Western Blotting

Non-polarized MDCK cells transfected with FM4-Rhodopsin-GFP were treated with AP21998 for the indicated times and lysed and subjected to Western blotting as described in (Wechselberger, Ebert et al. 2001). Briefly, lysates were subjected to SDS – polyacrylamide gel electrophoresis and proteins were transferred to PVDF membranes (Millipore Corporation). FM4-Rhodopsin-GFP was detected by an anti-GFP antibody, as loading control actin was detected by an anti-actin antibody.

Immunofluorescence

MDCK cells grown and treated as indicated were fixed for 15 min in 1 % Paraformaldehyde at room temperature and then permeabilized for 5 min in 0.1 % Triton X-100. After blocking in a solution containing 1 % bovine serum albumin (BSA) and 0.5 % Tween-20 cells were incubated with primary antibodies against the desired endogenous proteins and appropriate secondary antibodies conjugated to fluorescent dyes.

The following primary and secondary antibodies were used: Fig. 3A: anti-E-cadherin (BD Biosciences), anti-mouse-Alexa-647 (Invitrogen); Fig. 3B: anti-gp135 (provided by J. Fuellekrug, Univ. Heidelberg), anti-mouse-Alexa-647 (Invitrogen); Fig. 3C: anti-ZO-1 (Invitrogen), anti-mouse-Alexa-594 (Invitrogen); Figure 7B 0min: anti-calnexin, anti-mouse-Alexa-647 (Invitrogen); Figure 11: anti-Rab11 (Invitrogen), anti-rabbit-Alexa-568 (Invitrogen).

Nuclei were finally counterstained with either TO-PRO3 (Figs. 3A and 3B, Invitrogen) or DAPI (Figs. 3C, 7 and 11).

Manufacturing of version 1 of the biochip for apical TIRF microscopy

The chip consisted of two layers of poly(dimethylsiloxane) (PDMS; RTV 615 from Momentive) and was manufactured according to the method described in (Unger, Chou et al. 2000). The individual layers were manufactured by pouring (thicker layer; 5 A:1 B) or by spin-coating at 3500 rpm (thinner layer, 20 A:1 B) a PDMS pre-

polymer mixture of component A (PDMS bearing vinyl groups and a platinum catalyst) and component B (crosslinker containing silicon hydride groups) onto masters. The masters were polished silicon wafers (Siltronic) with features of photoresist on top. The photoresist features were manufactured by standard photolithography using photoresists from the SU-8 series (MicroChem). Masters were treated with trimethylchlorolosilane in order to prevent adhesion of the PDMS layer to the master during the next steps. After curing the PDMS layers for 30 min at 80 ℃ the thicker layer was cut to size, access holes to the actuator channel system were punched with 20 gauge needles and the thicker layer was aligned on the thinner layer. A second curing step at 90 ℃ over night ensured irreversible bonding of the two PDMS layers thereby forming the biochip.

Manufacturing of version 2 of the biochip for apical TIRF microscopy

The part of the chip containing the actuator channels (part 1) consisted of two layers of PDMS and was manufactured the same way as chip version 1. Part 1 of the chip was bonded to part 2 (support frame) and part 3 (central stamp, will carry later the cell layer) by pressing the parts together after activating the PDMS contact surfaces with plasma treatment. During this process the actuator channels were pressurized to ensure that part 3 bonded only to the upper part of the bulged membrane covering the actuator channels.

References

Axelrod, D. (2001). "Total internal reflection fluorescence microscopy in cell biology." Traffic **2**(11): 764-74.

Bonifacino, J. S. and L. M. Traub (2003). "Signals for sorting of transmembrane proteins to endosomes and lysosomes." Annu Rev Biochem **72**: 395-447.

Brown, D. (2003). "The ins and outs of aquaporin-2 trafficking." Am J Physiol Renal Physiol **284**(5): F893-901.

Brown, D. A. and E. London (1998). "Functions of lipid rafts in biological membranes." Annu Rev Cell Dev Biol **14**: 111-36.

Bryant, D. M., A. Datta, et al. (2010). "A molecular network for de novo generation of the apical surface and lumen." Nat Cell Biol **12**(11): 1035-45.

Bryant, N. J., R. Govers, et al. (2002). "Regulated transport of the glucose transporter GLUT4." Nat Rev Mol Cell Biol **3**(4): 267-77.

Capaldo, C. T. and I. G. Macara (2007). "Depletion of E-cadherin disrupts establishment but not maintenance of cell junctions in Madin-Darby canine kidney epithelial cells." Mol Biol Cell **18**(1): 189-200.

Casanova, J. E., X. Wang, et al. (1999). "Association of Rab25 and Rab11a with the apical recycling system of polarized Madin-Darby canine kidney cells." Mol Biol Cell **10**(1): 47-61.

Chen, W., Y. Feng, et al. (1998). "Rab11 is required for trans-golgi network-to-plasma membrane transport and a preferential target for GDP dissociation inhibitor." Mol Biol Cell **9**(11): 3241-57.

Chu, B. B., L. Ge, et al. (2009). "Requirement of myosin Vb.Rab11a.Rab11-FIP2 complex in cholesterol-regulated translocation of NPC1L1 to the cell surface." J Biol Chem **284**(33): 22481-90.

Chuang, J. Z. and C. H. Sung (1998). "The cytoplasmic tail of rhodopsin acts as a novel apical sorting signal in polarized MDCK cells." J Cell Biol **142**(5): 1245-56.

Cramm-Behrens, C. I., M. Dienst, et al. (2008). "Apical cargo traverses endosomal compartments on the passage to the cell surface." Traffic **9**(12): 2206-20.

Crane, J. M. and A. S. Verkman (2008). "Long-range nonanomalous diffusion of quantum dot-labeled aquaporin-1 water channels in the cell plasma membrane." Biophys J **94**(2): 702-13.

Cresawn, K. O., B. A. Potter, et al. (2007). "Differential involvement of endocytic compartments in the biosynthetic traffic of apical proteins." Embo J **26**(16): 3737-48.

Deborde, S., E. Perret, et al. (2008). "Clathrin is a key regulator of basolateral polarity." Nature **452**(7188): 719-23.

Desclozeaux, M., J. Venturato, et al. (2008). "Active Rab11 and functional recycling endosome are required for E-cadherin trafficking and lumen formation during epithelial morphogenesis." Am J Physiol Cell Physiol **295**(2): C545-56.

Diaz, F., D. Gravotta, et al. (2009). "Clathrin adaptor AP1B controls adenovirus infectivity of epithelial cells." Proc Natl Acad Sci U S A **106**(27): 11143-8.

Farr, G. A., M. Hull, et al. (2009). "Membrane proteins follow multiple pathways to the basolateral cell surface in polarized epithelial cells." J Cell Biol **186**(2): 269-82.

Gonzalez, A. and E. Rodriguez-Boulan (2009). "Clathrin and AP1B: key roles in basolateral trafficking through trans-endosomal routes." FEBS Lett **583**(23): 3784-95.

Hales, C. M., R. Griner, et al. (2001). "Identification and characterization of a family of Rab11-interacting proteins." J Biol Chem **276**(42): 39067-75.

Hammerton, R. W., K. A. Krzeminski, et al. (1991). "Mechanism for regulating cell surface distribution of Na+,K(+)-ATPase in polarized epithelial cells." Science **254**(5033): 847-50.

Hu, Q., L. Milenkovic, et al. (2010). "A septin diffusion barrier at the base of the primary cilium maintains ciliary membrane protein distribution." Science **329**(5990): 436-9.

Jaiswal, J. K. R., Victor M & Simon, Sanford M (2009). "Exocytosis of post-Golgi vesicles is regulated by components of the endocytic machinery." Cell **137**(7): 1308--1319.

Keller, P., D. Toomre, et al. (2001). "Multicolour imaging of post-Golgi sorting and trafficking in live cells." Nat Cell Biol **3**(2): 140-9.

Kessler, A., E. Tomas, et al. (2000). "Rab11 is associated with GLUT4-containing vesicles and redistributes in response to insulin." Diabetologia **43**(12): 1518-27.

King, L. S., D. Kozono, et al. (2004). "From structure to disease: the evolving tale of aquaporin biology." Nat Rev Mol Cell Biol **5**(9): 687-98.

Kock, I., N. A. Bulgakova, et al. (2009). "Targeting of Drosophila rhodopsin requires helix 8 but not the distal C-terminus." PLoS One **4**(7): e6101.

Kreitzer, G., J. Schmoranzer, et al. (2003). "Three-dimensional analysis of post-Golgi carrier exocytosis in epithelial cells." Nat Cell Biol **5**(2): 126-36.

Ladinsky, M. S., C. C. Wu, et al. (2002). "Structure of the Golgi and distribution of reporter molecules at 20 degrees C reveals the complexity of the exit compartments." Mol Biol Cell **13**(8): 2810-25.

Le Gall, A. H., S. K. Powell, et al. (1997). "The neural cell adhesion molecule expresses a tyrosine-independent basolateral sorting signal." J Biol Chem **272**(7): 4559-67.

Li, B. X., A. K. Satoh, et al. (2007). "Myosin V, Rab11, and dRip11 direct apical secretion and cellular morphogenesis in developing Drosophila photoreceptors." J Cell Biol **177**(4): 659-69.

Lock, J. G. and J. L. Stow (2005). "Rab11 in recycling endosomes regulates the sorting and basolateral transport of E-cadherin." Mol Biol Cell **16**(4): 1744-55.

Manders, E. M. M., F. J. Verbeek, et al. (1993). "Measurement of Colocalization of Objects in Dual-Color Confocal Images." Journal of Microscopy-Oxford **169**: 375-382.

Maxfield, F. R. and T. E. McGraw (2004). "Endocytic recycling." Nat Rev Mol Cell Biol **5**(2): 121-32.

Mellman, I. and W. J. Nelson (2008). "Coordinated protein sorting, targeting and distribution in polarized cells." Nat Rev Mol Cell Biol **9**(11): 833-45.

Nedvetsky, P. I., E. Stefan, et al. (2007). "A Role of myosin Vb and Rab11-FIP2 in the aquaporin-2 shuttle." Traffic **8**(2): 110-23.

Nejsum, L. N. and W. J. Nelson (2007). "A molecular mechanism directly linking E-cadherin adhesion to initiation of epithelial cell surface polarity." J Cell Biol **178**(2): 323-35.

Prekeris, R., J. Klumperman, et al. (2000). "A Rab11/Rip11 protein complex regulates apical membrane trafficking via recycling endosomes." Mol Cell **6**(6): 1437-48.

Rivera, V. M., X. Wang, et al. (2000). "Regulation of protein secretion through controlled aggregation in the endoplasmic reticulum." Science **287**(5454): 826-30.

Rodriguez-Boulan, E., G. Kreitzer, et al. (2005). "Organization of vesicular trafficking in epithelia." Nat Rev Mol Cell Biol **6**(3): 233-47.

Salvarezza, S. B., S. Deborde, et al. (2009). "LIM kinase 1 and cofilin regulate actin filament population required for dynamin-dependent apical carrier fission from the trans-Golgi network." Mol Biol Cell **20**(1): 438-51.

Satoh, A. K., J. E. O'Tousa, et al. (2005). "Rab11 mediates post-Golgi trafficking of rhodopsin to the photosensitive apical membrane of Drosophila photoreceptors." Development **132**(7): 1487-97.

Schmoranzer, J., M. Goulian, et al. (2000). "Imaging constitutive exocytosis with total internal reflection fluorescence microscopy." J Cell Biol **149**(1): 23-32.

Simmen, T., M. Nobile, et al. (1999). "Basolateral sorting of furin in MDCK cells requires a phenylalanine-isoleucine motif together with an acidic amino acid cluster." Mol Cell Biol **19**(4): 3136-44.

Steyer, J. A. and W. Almers (2001). "A real-time view of life within 100 nm of the plasma membrane." Nat Rev Mol Cell Biol **2**(4): 268-75.

Steyer, J. A., H. Horstmann, et al. (1997). "Transport, docking and exocytosis of single secretory granules in live chromaffin cells." Nature **388**(6641): 474-8.

Sung, C. H. and J. Z. Chuang (2010). "The cell biology of vision." J Cell Biol **190**(6): 953-63.

Tai, A. W., J. Z. Chuang, et al. (1999). "Rhodopsin's carboxy-terminal cytoplasmic tail acts as a membrane receptor for cytoplasmic dynein by binding to the dynein light chain Tctex-1." Cell **97**(7): 877-87.

Tai, A. W., J. Z. Chuang, et al. (2001). "Cytoplasmic dynein regulation by subunit heterogeneity and its role in apical transport." J Cell Biol **153**(7): 1499-509.

Tan, W., A. L. Oldenburg, et al. (2006). "Optical coherence tomography of cell dynamics in three-dimensional tissue models." Opt Express **14**(16): 7159-71.

Tenstad, E., A. Tourovskaia, et al. (2010). "Extensive adipogenic and osteogenic differentiation of patterned human mesenchymal stem cells in a microfluidic device." Lab Chip.

Toomre, D., J. A. Steyer, et al. (2000). "Fusion of constitutive membrane traffic with the cell surface observed by evanescent wave microscopy." J Cell Biol **149**(1): 33-40.

Tucker, T. A., K. Varga, et al. (2003). "Transient transfection of polarized epithelial monolayers with CFTR and reporter genes using efficacious lipids." Am J Physiol Cell Physiol **284**(3): C791-804.

Ullrich, O., S. Reinsch, et al. (1996). "Rab11 regulates recycling through the pericentriolar recycling endosome." J Cell Biol **135**(4): 913-24.

Unger, M. A., H. P. Chou, et al. (2000). "Monolithic microfabricated valves and pumps by multilayer soft lithography." Science **288**(5463): 113-6.

Wang, X., R. Kumar, et al. (2000). "Regulation of vesicle trafficking in madin-darby canine kidney cells by Rab11a and Rab25." J Biol Chem **275**(37): 29138-46.

Wechselberger, C., A. D. Ebert, et al. (2001). "Cripto-1 enhances migration and branching morphogenesis of mouse mammary epithelial cells." Exp Cell Res **266**(1): 95-105.

Weisz, O. A. and E. Rodriguez-Boulan (2009). "Apical trafficking in epithelial cells: signals, clusters and motors." J Cell Sci **122**(Pt 23): 4253-66.

Wellner, R. B. and B. J. Baum (2001). "Polarized sorting of aquaporins 5 and 8 in stable MDCK-II transfectants." Biochem Biophys Res Commun **285**(5): 1253-8.

Wu, S., S. Q. Mehta, et al. (2005). "Sec15 interacts with Rab11 via a novel domain and affects Rab11 localization in vivo." Nat Struct Mol Biol **12**(10): 879-85.

Yeh, T. Y., D. Peretti, et al. (2006). "Regulatory dissociation of Tctex-1 light chain from dynein complex is essential for the apical delivery of rhodopsin." Traffic **7**(11): 1495-502.

Zerial, M. and H. McBride (2001). "Rab proteins as membrane organizers." Nat Rev Mol Cell Biol **2**(2): 107-17.